Kinematic Analysis and Dimensional Synthesis of a Meso-Gripper

Guochao Bai
Institute of Mechanical, Process & Energy Engineering,
School of Engineering and Physical Sciences,
Heriot-Watt University,
Edinburgh, Scotland, UK EH14 4AS
e-mail: gb9@hw.ac.uk
ASME Student Member

Xianwen Kong[1]
Institute of Mechanical, Process & Energy Engineering,
School of Engineering and Physical Sciences,
Heriot-Watt University,
Edinburgh, Scotland, UK EH14 4AS
e-mail: X.Kong@hw.ac.uk
ASME Member

James Millar Ritchie
Institute of Mechanical, Process & Energy Engineering,
School of Engineering and Physical Sciences,
Heriot-Watt University,
Edinburgh, Scotland, UK EH14 4AS
e-mail: J.M.Ritchie@hw.ac.uk

ABSTRACT

In recent years, applications in industrial assemblies within a size range from 0.5mm to 100mm are increasing due to the large demands for new products, especially those associated with digital multimedia. Research on grippers or robotic hands within the mesoscopic scale of this range has not been explored in any great detail. This paper outlines the development of a gripper to bridge the gap between micro-grippers and macro-grippers by extending the gripping range to the mesoscopic scale, particularly without the need to switch grippers during industrial assembly. The mesoscopic scale gripper (meso-gripper) researched in this work has two modes of operation: passive adjusting and an angled gripping, adapting

[1] Corresponding author.

its configuration to the shape of object automatically. This form of gripping and the associated mechanism are both novel in their implementation and operation. Firstly, the concept of mesoscopic scale in robotic gripping is presented and contextualized around the background of inefficient hand switching processes and applications for assembly. The passive adjusting and angled gripping modes are then analyzed and a dual functional mechanism design proposed. A geometric constraint method is then demonstrated which facilitates task-based dimensional synthesis after which the kinematics of synthesized mechanism is investigated. The modified synthesized mechanism gripper is then investigated according to stiffness and layout. Finally, a 3D printed prototype is successfully tested and the two integrated gripping modes for universal gripping verified.

Key words: meso-scale, passive adjusting, angled gripping, metamorphic, dimensional synthesis

1 INTRODUCTION

Grippers and robotic hands are essential and important end-effectors of robotic manipulators. The development of grippers or robotic hands able to pick up objects for different applications has attracted much attention within the research community over the last four decades. Grippers vary from simple configurations, such as two-jaw parallel designs, to complex, hand-like shapes with advanced sensors, control units and servomotors. The initial type of gripper application used in industry was for picking up raw and finished parts [1]. The majority of grippers are variations of three fundamental designs, namely: parallel, three-fingered, and angled grippers. A two-finger gripper has the minimum number of fingers and the minimum complexity of a hand. According to typical types of industrial gripper applications, the minimum gripping force of a parallel gripper is difficult to control especially for small loads. Angled grippers can be adjusted

to various angles according to work piece and space limitations. Also, robotic grippers that mimic anthropomorphic hands have also been investigated and applied in industry. Within such systems, fingers are the most important components of a precision grasping "hand" [2]. These can mainly be classified into three types: low-cost grippers for industrial production, precision grasping and under-actuated grasping [3]. Recent research on universal high flexibility, multi-functional robotic grippers has been carried out and some systems have been developed [4]. However, it is still difficult to grip very small, fragile and light objects with such grippers. With the development of microscale technologies in electronics, optics and biology, micro-grippers are required for microrobot and microassembly. Micro-grippers also require to grip and handle the micro-objects securely and accurately with the range below 100μm, preferably with no gripper changes. Some specifically designed micro-grippers handle objects ranging from nanometers up to 500μm. In a variety of circumferences a robot has to switch hands for gripping objects with different sizes, shapes and ranges of gripping force that requires. A general purpose "hand" that can accomplish all of these tasks will make gripping much more efficient and reduce changeover times.

To address this gap, in this research a meso-gripper which has metamorphic characteristics and two gripping modes shown in Fig. 1 is proposed, developed and tested.

Fig. 1 Prototype of a meso-gripper with two gripping modes

This paper is organized as follows. In Sec. 2, a meso-scale for gripping technology is defined according to human grasping behaviors and processes. The gripper is then

designed and developed by integrating a remote center of motion (RCM) mechanism with a cross four-bar (CFB) linkage. In Sec. 3, the dimensional synthesis of the gripper is outlined for a specified gripping task followed by analysis of the synthesizing mechanism. In Sec. 4 the design is modified via 3D model by considering stiffness and layout of the assembly and a differential mechanism included to increase the gripper flexibility. In Sec. 5, from the model a physical prototype is fabricated using 3D printing and manually tested to evaluate and verify the feasibility of the gripper design. The paper then concludes with the further consideration of gripping forces during the design process and comments on the outcomes and future direction of research.

2 GRIPPING PROCESS ANALYSIS AND ASSOCIATED MECHANISM DESIGN INSPIRATION

2.1 The definition of meso-scale in robotic gripping

Generally speaking, the mesoscopic scale comprises different length scales in different research areas. A comparison of the relevant length scales in material science and molecular biology shows that the mesoscopic length is 10^6-10^8 nm (1-100mm) [5]. However, some specifically designed micro-grippers handle objects up to 500µm; therefore the minimum gripping size of a meso-gripper has been defined in this work as 500µm. A meso-gripper bridges the gap between micro-grippers and macro-grippers by extending the macro-gripping range, preferably without switching grippers for industrial assembly. Therefore in Fig. 2, this work defines the working gripping dimension range of

meso-grippers as from 0.5 to 100mm, based on typical requirements for the assembly of multimedia products.

Fig. 2 Schematic comparison of the length scales in material science, gripping technology and molecular biology

2.2 Analysis of gripping process

Two manual gripping examples were considered and various configurations of fingers observed to help define the functionality of the proposed meso-gripper. These examples comprise two parts, a very thin hex socket screw with a diameter of 1.5mm and a plastic cuboid with dimensions 28mm × 24mm × 17 mm. Both were observed to be processed in four steps, namely: searching, reaching, gripping and moving [6] (see Fig. 3). The objective for each step in assembling these two parts is the same but the configurations are different due to size and shapes of the parts.

The gripping process of hex socket is as follows:

a. Distal segments of thumb and index fingers contact each other, then move to the hex socket.

b. The contacted fingers reach above the hex socket.

c. The hex socket is gripped by fingertips.

d. The hex socket is moved.

The gripping process for plastic cuboid is

a. The thumb and index fingers move to the plastic cuboid.

b. Distal segments of thumb and index fingers reach and contact two edges of the cuboid.

c. Pads of thumb and index fingertips grip the sides of the part for clamping.

d. The cuboid is moved.

Comparing these two processes, gripping the hex socket screw requires only one degree of freedom (DOF) while gripping the cuboid requires two DOFs (see Fig. 3). This analysis greatly simplifies the finger design for gripping these objects. Two DOFs, one for positioning and another for clamping, are the minimum number of DOF required in these gripping processes.

Fig. 3 Gripping processes for hex socket and plastic cuboid

2.3 CFB mechanism for passive adjusting and angled gripping

Gripping using a human hand is activated because the neural and visual systems work as sensors with the brain operating as a control system. According to the gripping analysis in Sec. 2.2, 2-DOF fingers could be adopted to grip meso-scale parts in two modes. The key challenge is to build a 2-DOF finger with two gripping modes. Therefore, a passive adjusting concept was proposed in this section for gripping meso-scale parts.

Progress in research and development for grippers has been made in underactuated grasping; for example, Birglen and Gosselin have used a five-bar linkage and a four-bar linkage connected in series to design three-phalanx underactuated fingers [7]. Ceccarelli et al have designed three-phalanx underactuated fingers with CFB linkage in series [8]. To create stable, encompassing grasps with subsets of fingers, soft fingertips that deform during contact and apply a larger special spread of frictional forces and moments than their rigid counterparts have been studied [9]. CFB linkage is found to be good candidates to achieve passive-adjusting motion and has similar characteristics as

to soft fingertip. Passive adjusting mechanism has characteristics such as adaptivity, under-actuativity, efficiency and multifunction whereby such a system can adjust itself automatically depending on the locations and shapes of objects.

A CFB linkage is shown in Fig. 4(a). Crank link AD rotates from initial angle γ with respect to vertical line to angle γ' the coupler link CD reaches position. In turn, the mechanism can adjust passively when one point of link CD contacts an object. If the positions of two points of the coupler link CD are determined, the configuration of the whole mechanism will be fixed. A soft-fingertip model composing with CFB-damper-spring component is shown in Fig. 4(b). Friction is represented as f at the fingers' contact surfaces. The normal force applied on the each fingertip is F_n. The mass of object and mass of CFB linkage is G_m and G_l respectively. K_s and R_d represent the stiffness of the spring and damper ratio respectively. Analysis of contact positions should be conducted before applying it as a fingertip for gripping. Furthermore if the motion of one endpoint of link CD contacts with the symmetrical side then these two CFB mechanisms will be angled fingertips.

Fig. 4 CFB mechanism as passive adjusting fingertip

2.4 RCM mechanism for positioning

RCM mechanisms are widely used as a wrist for a minimally invasive surgery (MIS) robot to provide a fixed point moving around the surgical incision. An RCM manipulator was first developed by Taylor et al [10], then the concept and mechanism were used in MIS for precision operations as a steady hand [11]. Bai expanded the mechanism to multiple RCMs for complicated applications by investigating the relationship between RCM

mechanism and deployable mechanism. A multiple RCM mechanism [12] was proposed and some applications, such as foldable stages and a surgical helmet for ophthalmology, were demonstrated in [13]. The kinematic analysis of the RCMs shows that the end link of the mechanism has the same rotation angle as the drive link no matter how many links are connected between them. As shown in Fig. 5, links HJ and GE rotate around two remote centers O1 and O2 respectively and have the same rotational angles as the drive link AC [13]. This characteristic makes the mechanism useful and easily controllable. In this paper, an RCM mechanism will be used as a middle and proximal phalanx to provide gripping force and clamping motion.

Fig. 5 Dual RCM mechanism

2.5 The integrated mechanism

The overall gripper model was obtained by integrating the RCM, CFB mechanisms, damper and spring. The gripping process mimics the human hand as shown in Fig. 6. The process shows that the integrated mechanism passively adapts to parallel sides of a cuboid.

Fig. 6 Sequential gripping process of the integrated mechanism

2.6 Metamorphic gripping

Considerable development in theoretical research on metamorphic mechanisms [14] has been made in the past 15 years such as the metamorphic hand [15] and walking machines. The meso-gripper during passive adjusting mode shown in Fig. 7(a) has two DOFs when considering one side of the gripper. The DOF of the mechanism will reduce

to one if one point of CFB mechanism touches the object. If two points of the coupler link of the CFB linkage touch the object, the DOF degrades to -1, i.e. it is over-constrained. Therefore, the meso-gripper is an example of metamorphic mechanism. A detailed analysis of this characteristic is outlined below.

The process of cuboid gripping is similar to the four steps shown in Fig. 3. The object M is supposed to be fixed to the frame while point I of the CFB mechanism slides on the surface of the object until point H contacts it as shown in Fig. 7(a). The solid line diagram shows the point at which the mechanism reaches the cuboid and the dashed diagram the final configuration. The equivalent mechanism during the gripping process is shown in Fig. 7(b). The DOF (F) analysis of this mechanism during this process is calculated as follows using Gruebler's equation where n = number of moving links, p_l = number of lower pairs, p_h = number of higher pairs:

Searching step: $F=3n-2p_l-2p_h=3x8-2x11=24-22=2$

Reaching step: $F=3n-2p_l-2p_h=3x9-2x13=27-26=1$

Gripping step: $F=3n-2p_l-2p_h=3x7-2x11=21-22=-1$

The number of movable links of the mechanism changes during the gripping process, causing a subsequent change in its topology.

Fig. 7 Metamorphic gripping and equivalent mechanism

The angled gripping mode of the gripper has a similar motion to the passive adjusting mode. The DOFs and topology of the mechanism vary at different gripping steps.

3 DIMENSIONAL SYNTHESIS AND KINEMATIC ANALYSIS

Geometric constraint programming was proposed to solve general kinematic synthesis problem, such as planar four-bar linkages for motion generation, path generation and function generation [16]. Detailed dimensional synthesis and kinematic analysis of the multi-RCM mechanism can be found in [12, 13]. The design process of the meso-gripper using this approach will be presented in this section.

3.1 Task-based dimensional synthesis

The objective of dimensional synthesis is to determine the value of each geometric parameter of a mechanism by taking account of its desired performance. Geometric parameters vary with the design criteria. Gripping range is one of the most important criteria which differentiate the meso-gripper from other designs. The dimensions of the mechanism will be presented based on the task requirements.

A geometrical constraint approach is presented to help design mechanisms over a specific gripping range. The approach is closely related to the synthesis of multi-RCM mechanisms [12]. The differences mainly lie in the prototype design and manufacturing considerations.

The task requirements specification is as follows:

(1) The gripping range of the meso-gripper should be 0-55mm.

(2) The range of angled gripping mode is 0-6mm.

(3) The range of passive adjusting mode is 6-55mm.

(4) The mechanism of gripper should be compact.

The synthesis process incorporating the geometrical constraint approach is outlined as follows:

Step 1. Determination of initial positions according to the task requirements: Fig. 8 gives an enlarged range of 0-60mm for the optimization. The RCM point and the first frame point are determined by considering the compactness of the whole gripper.

Fig. 8 Objective gripping range and key points

Step 2. Design of the CFB linkage: The dimensions of CFB linkage are shown in Fig. 9. The length of follower link should be longer than crank link to build angled configuration for angled gripping. The connecting link will connect to the RCM mechanism.

Fig. 9 CFB linkage with integer dimensions

Step 3. Determination of position at angled gripping mode: The CFB linkage is incorporated into the graph obtained from Step 1. The length of drive link is set at 40mm i.e. larger than 30mm which is at the borderline limit. A circle of 40mm radius is drawn with the RCM point its center. The two endpoints of the coupler link are positioned on the symmetrical line and 3mm borderline respectively. One endpoint of connecting link is placed on the circle and a line drawn from the RCM point to the end of the circle, making the angle between it and connecting link of the CFB linkage 150°. The position of CFB linkage at the angled gripping mode is then determined, as shown in Fig. 10.

Fig. 10 Position determination of CFB linkage

Step 4. Determination of position at initial passive adjusting mode: As is shown in Fig. 11, one end of the coupler link is positioned at the 30mm borderline, connecting one endpoint of the connecting link at the circle. This makes the angle between the connecting link and the RCM line 150°.

Fig. 11 Initial position of CFB linkage

Step 5. Synthesis of the RCM mechanism: By using synthesis method of the RCM mechanism [12], the dimensions of the RCM mechanism can be determined. Based on the first frame point, the second frame point with a frame dimension of 10mm and a 135° angle is drawn about the horizontal line. Parallelogram 1 is constructed according to the two-point frame line and drive link. Parallelogram 2 is constructed using the connecting link and the RCM position line. Based on these two parallelograms, parallelogram 3 is then determined as shown in Fig. 12.

Fig. 12 Synthesis of initial position of mechanism

Step 6. Verification: Three angles should be verified to determine the feasibility of the synthesized mechanism. If angle δ is larger than ϑ then the synthesized mechanism can reach the pre-set position as shown in Fig. 13. Angle Ψ should be no greater than 90° to make the 55mm object gripping successful. In Fig. 13 angle Ψ is greater than 90°, so a modification should be made.

Fig. 13 Verification of designed mechanism

Step 7. Optimization: The initial position of the RCM mechanism is changed in order to reduce the verification angle Ψ to 90° by rotating the crank link of CFB mechanism as shown in Fig. 14. As a consequence, the final design meets the maximum gripping size requirement of 55mm.

Fig. 14 Final design after verification

3.2 Kinematic analysis of designed mechanism

In order to verify the parameters of the synthesized mechanism, kinematic analysis of the mechanism is carried out. The most important geometric parameters are the drive angle and the motion between contact surface and the object. Two different modes of gripping: passive adjusting and angled gripping are analyzed in this section. The rotating angle of driving link and the distance moved by point I on the contacting surface are the basic parameters required for further design of the drive method and the subsequent gripping force analysis.

As is shown in Fig. 15, the solid line diagram shows the final position for gripping a 55mm object and the dashed line diagram shows the initial position of the mechanism. Point I slides on the object surface using a slide link as shown. It is determined that the rotating angle (*RA*) of the drive link is 6.42° and slide distance of point I about y axis (*Uy*) is 4.3mm.

Fig. 15 Gripping a 55mm object during passive adjusting mode (a) Equivalent schematic; (b) Range of rotating angle of drive link AC and sliding distance of point I

As shown in Fig. 16, the gripping process for an object of 6mm requires a maximum *RA* of drive link AC of around 2.9° and contacting point I sliding around 1.28mm

Fig. 16 Gripping an object of less than 6mm at angled mode. (a) Equivalent schematic; (b) Range of rotating angle of drive link AC and sliding distance of point I

4 MODIFIED DESIGN AND 3D MODELING

In Sec. 3, a geometrical constraint method was presented to design a gripper for a reqiured gripping range. Kinematic analysis of the mechanism helps an understanding of the gripping process and determines the drive position. In this section, modified design

is presented by considering stiffness of the mechanism and layout of the assembly for prototyping and manufacturing.

4.1 Modified schematic of the gripper

As shown in Fig. 17(b), the integrated mechanism has four layers at the position of cross four-bar mechanism because of its multiple joints. This layout leads to the tip of the gripper being less stiff for accelerated gripping. So it is more advantageous to reduce the layers of the mechanism to provide a smaller gripping torque at the tip linkages.

Fig. 17 Layout of the assembly of meso-gripper

The CFB mechanism should be modified by changing the multiple joint of connecting link into a single joint with the coupler link of the mechanism reduced in size to provide adequate space for tip contact surface.

Fig. 18 Modified schematic considering layers and contact surfaces

Figures 19 and 20 show the kinematics of the meso-gripper at passive adjusting and angled gripping modes. The rotating angles of drive link at these two modes are around 8.65° and 2.91° and sliding distances of contacting point I are 2.94mm and 1.24mm respectively.

Fig. 19 Kinematic analysis of the meso-gripper at passive adjusting mode

Figure 20. Kinematic analysis of the meso-gripper at angled mode

4.2 Modified RCM mechanism

A typical RCM mechanism comprises a 6-bar over-constraint mechanism containing 3-parallelogram loops as shown in Fig. 21(a). The mechanism transfers to one DOF by

removing one connecting link of the parallelogram loop as shown in Fig. 21(b). However, this simplification reduces the stiffness of the mechanism because one supporting link is removed. At passive adjusting mode, the weight of the object and associated acceleration may result in a very large torque on some links; meanwhile the meso-gripper must be designed to be compact with each component being very small. This requires that the stiffness of the whole mechanism must be considered. Jensen [17] provided a design with pulley coaxial with the pivot by fixing connecting links on the pulley wheel as shown in Fig. 22(a). Tendon- or belt- actuated mechanisms are limited to small gripping forces and lead to increased friction and elasticity. In this section an alternative approach to increase the stiffness of RCM mechanism is proposed by using redundant links as detailed in Fig. 22(b).

Fig. 21 Simplification of RCM mechanism

Fig. 22 Pulley-driven mechanism and the equivalent mechanism

The modified RCM mechanism is developed in Fig. 23(a). Due to its geometric characteristics, the dimensions of the mechanism are determined by simplifying the angulated link, as shown in Fig. 23(b).

Fig. 23 Modified schematic and 3D drawing of RCM

4.3 Modified cross four-bar linkage

A CFB linkage is used for passive adjustment due to the complicated contacting surfaces. References [18, 19] propose a method to exactly duplicate the kinematic characteristics of a rigid-link four-bar mechanism by using the centrodes of the four-bar linkage. A mechanism that is overconstrained may be the best choice in problems of machine

design when larger and variable loads must be sustained by means of mass and compliance, especially when the maintenance of mechanical accuracy is important [20]. The continuous trajectories of fixed and moving centrodes are the contact-aided surfaces for exactly duplicating the kinematic characteristics of rigid four-bar linkage.

Fig. 24 Relative angles of connecting and crank links for passive adjusting and angled gripping modes

According to kinematic analysis shown in Fig. 24, the drive angles of crank links are calculated as 18.06° and 5.65° for adjusting and angled modes individually. The larger angle of 18.06° should be selected to generate trajectories of fixed and moving centrodes of modified CFB mechanism.

Fig. 25 Initial and final positions of modified CFB Mechanism

Initial and final positions of the modified CFB mechanism are obtained while trajectories of fixed and moving centrodes of the mechanism are generated. By copying corresponding files of the trajectories to 3D modeling software, the over-constrained mechanism considering dimensions of crank and connecting links is generated as shown in Fig. 25(c).

4.4 Drive approach design

The concept of underactuation [21] in robotic gipping with fewer actuators than DOFs allows the two fingers to adjust to irregular shapes without the need for complex control strategies and sensors. Differential mechanisms are used in robotic hands to provide underactuation, such as a movable pulley, seesaw mechanism, fluidic T-pipe and planetary and bevel gear differentials [22]. In this paper two fingers are driven by a

movable pulley for irregular shapes, as shown in Fig. 26(a). This differential system locates at the palm of the gripper with the two ends of the tendon are fixed symmetrically in the two fingers' pulley wheels, as shown in Fig. 26 (b). The actuated power is distributed to the two fingers to facilitate gripping of non-centered or irregularly shaped objects.

Fig. 26 Movable pulley for underactuated drive

4.5 3D modeling

The final 3D model of the meso-gripper with integrate design passive adjusting and angled gripping modes is shown in Fig. 27. The whole design was scaled up to 200% for better 3D printing. The gripping range for passive adjusting mode is 12-110mm and for angled gripping mode 0-12mm.

Fig. 27 Meso-gripper with two modes

5 MESO-GRIPPER PROTOTYPE AND TEST

Most of the components of the gripper were manufactured using 3D printing. The material used for gripper body is polylactide thermoplastic (PLA). For the coupler link of CFB linkage a silicone elastomer was used. The prototype of the gripper can grip different objects manually using both modes.

As shown in Fig. 28, objects used for testing the gripper's gripping capabilities include regular shapes (cylinder, cone, hexagon) and irregular shapes (flat, sharp and pinecone). The sizes of these objects varied from 0.5 to 105mm with gripping loads varying from 0.5 to 1000g. For different types of objects the gripping approach was different, e.g.

vertical gripping, horizontal gripping, passive adjusting mode gripping or angled gripping. In all cases the meso-gripper performed successfully.

Fig. 28 Gripping tests for different objects

6 CONCLUSIONS

This paper has introduced the concept and defined the range of the meso-scale for robotic gripper design as well as formalization of a methodology for such a gripping system. It has also demonstrated and validated this methodology through the design, analysis and testing of a meso-gripper combining two integrated operational modes, passive adjusting and angled gripping.

By focusing on the gripping process of the human hand, this integrated RCM mechanism and CFB linkage was developed using a geometrical constraint approach for dimensional synthesis of the mechanism. The kinematics of the synthesized mechanism were analyzed for model designed. The modified design considering stiffness and layout of the mechanism generated a new model. A 3D-printed manually operated prototype was tested for gripping different types of objects. The result shows the gripper with passive adjusting and angled gripping modes can achieve universal gripping within the meso-scale as scales as small as 0.5mm with a gripping load of as little as 0.5g. The general purpose meso-gripper successfully addresses the gap identified in the introduction. Future research will consider the gripping force during dimensional synthesis. Sensors attached to the fingertip will be used to measure the gripping force imposed on objects in the gripper control.

ACKNOWLEDGMENT

The authors would like to thank the Engineering and Physical Sciences Research Council (EPSRC), United Kingdom, for the support under grant No EP/K018345/1 and the first author would also like to thank the international Doctoral Training Partnership (DTP) from the EPSRC.

NOMENCLATURE

f	friction
Fn	force applied to finger tip
G_m	mass of object m
G_i	mass of mechanism
K_s	stiffness of the spring
R_d	damper ratio
F	degree of freedom
n	number of moving links
p_l	number of lower pairs
p_h	number of higher pairs
δ	angle between two links in parallelogram
ϑ	angle RCM link at initial and final position
Ψ	angle between couple link in CFB mechanism and vertical line
RA	rotating angle
Uy	slide distance of point I about y axis
meso-gripper	mesoscopic scale gripper
RCM	remote center of motion

CFB	cross four-bar
DOF	degree of freedom
MIS	minimally invasive surgery
PLA	polylactide thermoplastic

REFERENCES

[1] Lundström, G., 1974, "Industrial Robot Grippers," Industrial Robot: An International Journal, **1**(2), pp. 72-82.

[2] Li, G., Zhang, C., Zhang W., Sun Z., Chen, Q., 2014. "Coupled and Self-Adaptive Under-Actuated Finger With a Novel S-Coupled and Secondly Self-Adaptive Mechanism," Journal of Mechanisms and Robotics, **6**(4), 041010.

[3] Laliberté, T., and Gosselin, C. M., 1998, "Simulation and Design of Underactuated Mechanical Hands," Mechanism and Machine Theory, **33**(1), pp. 39-57.

[4] Brown, E M., Amend, J R. and Rodenberg, N., 2011, "A Positive Pressure Universal Gripper Based on the Jamming of Granular Material," IEEE Transactions on Robotics, **28**, pp. 341-350.

[5] Steinhauser, M. O., Hiermaier, S., 2009, "A Review of Computational Methods in Materials Science: Examples from Shock-Wave and Polymer Physics," International Journal of Molecular Sciences, **10**(12), pp.5135-5216.

[6] Niebel, B. W., 1993, "Motion and Time Study" Published by Richard D Irwin, pp. 197-205.

[7] Birglen., L, Gosselin. C. M., 2005, "Geometric Design of Three-Phalanx Underactuated Fingers," Journal of Mechanical Design, **128**(2), pp.356-364.

[8] Ceccarelli, C. M., Tavolieri, C., Lu, Z., 2006, "Design Considerations for Underactuated Grasp with a One DOF Anthropomorphic Finger Mechanism," In: Proceedings of the 2006 IEEE/RSJ International Conference on Intelligent Robots and Systems, Beijing, pp.1611-1616.

[9] Khurshid, A., Ghafoor, A., Malik, M. A., 2011, "Robotic Grasping and Fine Manipulation Using Soft Fingertip," Advances in Mechatronics, pp.155-174.

[10] Taylor, R. H., Funda, J., Larose, D., Michael Treat, M. D., 1992, "A Telerobotic System for Augmentation of Endoscopic Surgery," In: 14th IEEE Conference on Engineering in Medicine and Biology Society, Paris, France, pp.1054-1056.

[11] Taylor, R. H., Jenson, P., Whitcomb, L., Barnes, A., Kumar, R., Stoianovici, D., Gupta, P., Wang, Z., Dejuan, E., Kavoussi, L., 1999, "A Steady Hand Robotic System for Microsurgical Augmentation," International Journal of Robotics Reasearch, **18**(12), pp.1201-1210.

[12] Bai, G., Li, D., Wei, S., Liao, Q., 2014, "Kinematics and Synthesis of a Type of Mechanisms with Multiple Remote Centers of Motion," Proceedings of the Institution of Mechanical Engineers, Part C: Journal of Mechanical Engineering Science, **228**(18), pp. 3430-3440.

[13] Bai, G., Qi, P., Althoefer, K., Li, D., Kong, X., Dai, J. S., 2015, "Kinematic Analysis of a Mechanism With Dual Remote Centre of Motion and its Potential Application," ASME 2015 International Design Engineering Technical Conferences and Computers and Information in Engineering Conference, Boston, Massachusetts, USA, pp. V05BT08A011.

[14] Dai, J. S., and Jones, J. R., 1999, "Mobility in metamorphic mechanisms of foldable/erectable kinds," Journal of Mechanical Design, **121**(3), pp. 375-382.

[15] Dai, J. S., Wang, D., 2006, “Geometric Analysis and Synthesis of the Metamorphic Robotic Hand,” Journal of Mechanical Design, **129**(11), pp.1191-1197.

[16] Kinzel, Edward C., James P. Schmiedeler, and Gordon R. Pennock. 2006, "Kinematic synthesis for finitely separated positions using geometric constraint programming," Journal of Mechanical Design, **128**(5), pp. 1070-1079.

[17] Jensen, J. F., 2005, “Remote center positioner,” CA, US20050119638.

[18] Moon Y., 2007, “Bio-mimetic design of finger mechanism with contact aided compliant mechanism,” Mechanism and Machine Theory, **42**(5), pp. 600-611.

[19] Bai, G., Wang, J., Kong, X., 2016, “A Two-Fingered Anthropomorphic Robotic Hand with Contact-Aided Cross Four-Bar Mechanisms as Finger Joints,” Biomimetic and Biohybrid Systems: 5th International Conference, Living Machines 2016, Edinburgh, UK, pp. 28-39.

[20] Phillips, J., 2007, “Freedom in Machinery”. 1st ed. Cambridge: Cambridge University Press.

[21] Laliberté, T., and Gosselin, C. M., 1998, "Simulation and Design of Underactuated Mechanical Hands," Mechanism and Machine Theory, **33**(1), pp.39-57.

[22] Lionel, B., and Gosselin, C. M., 2006, "Force Analysis of Connected Differential Mechanisms: Application to Grasping," The International Journal of Robotics Research, **25**(10), pp. 1033-1046.

Figure Captions List

Fig. 1 Prototype of a meso-gripper with two gripping modes

Fig. 2 Schematic comparison of the length scales in material science, gripping technology and molecular biology

Fig. 3 Gripping processes for hex socket and plastic cuboid

Fig. 4 CFB mechanism as passive adjusting fingertip

Fig. 5 Dual RCM mechanism

Fig. 6 Sequential gripping process of the integrated mechanism

Fig. 7 Metamorphic gripping and equivalent mechanism

Fig. 8 Objective gripping range and key points

Fig. 9 CFB linkage with integer dimensions

Fig. 10 Position determination of CFB linkage

Fig. 11 Initial position of CFB linkage

Fig. 12 Synthesis of initial position of mechanism

Fig. 13 Verification of designed mechanism

Fig. 14 Final design after verification

Fig. 15 Gripping a 55mm object during passive adjusting mode: (a) equivalent schematic, (b) range of *RA* of drive link AC and sliding distance of point I

Fig. 16 Gripping an object of less than 6mm at angled mode: (a) equivalent

schematic, (b) range of *RA* of drive link AC and sliding distance of point I

Fig. 17 Layout of the assembly of meso-gripper

Fig. 18 Modified schematic considering layers and contact surfaces

Fig. 19 Kinematic analysis of the meso-gripper at passive adjusting mode

Fig. 20 Kinematic analysis of the meso-gripper at angled mode

Fig. 21 Simplification of RCM mechanism

Fig. 22 Pulley-driven mechanism and the equivalent mechanism

Fig. 23 Modified schematic and 3D drawing of RCM

Fig. 24 Relative angles of connecting and crank links for passive adjusting and angled gripping modes

Fig. 25 Initial and final positions of modified CFB Mechanism

Fig. 26 Movable pulley for underactuated drive

Fig. 27 Meso-gripper with two modes

Fig. 28 Gripping tests for different objects

Fig.1

(a) Passive adjusting mode

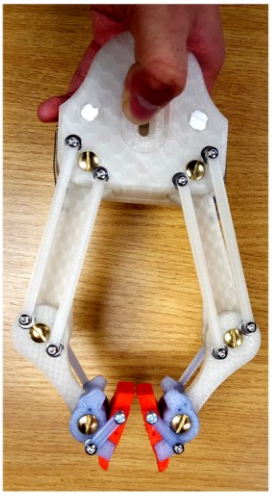

(b) Angled gripping mode

Fig. 2

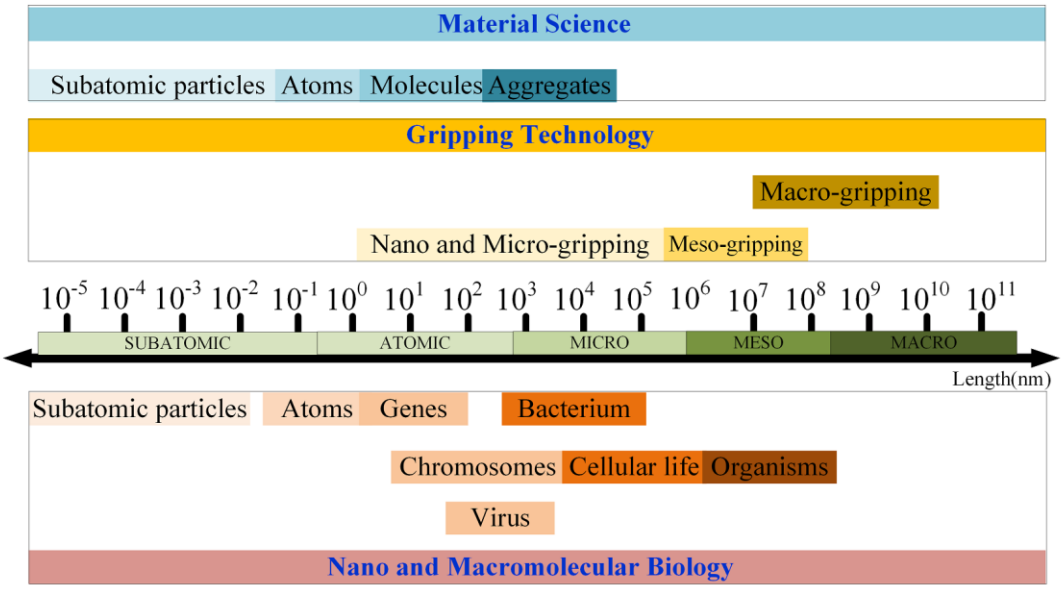
Material Science
Subatomic particles
Atoms
Molecules
Aggregates
Gripping Technology
Macro-gripping
Nano and Micro-gripping
Meso-gripping
10^{-5} 10^{-4} 10^{-3} 10^{-2} 10^{-1} 10^{0} 10^{1} 10^{2} 10^{3} 10^{4} 10^{5} 10^{6} 10^{7} 10^{8} 10^{9} 10^{10} 10^{11}
SUBATOMIC
ATOMIC
MICRO
MESO
MACRO
Length(nm)
Subatomic particles
Atoms
Genes
Bacterium
Chromosomes
Cellular life
Organisms
Virus
Nano and Macromolecular Biology

Fig. 3

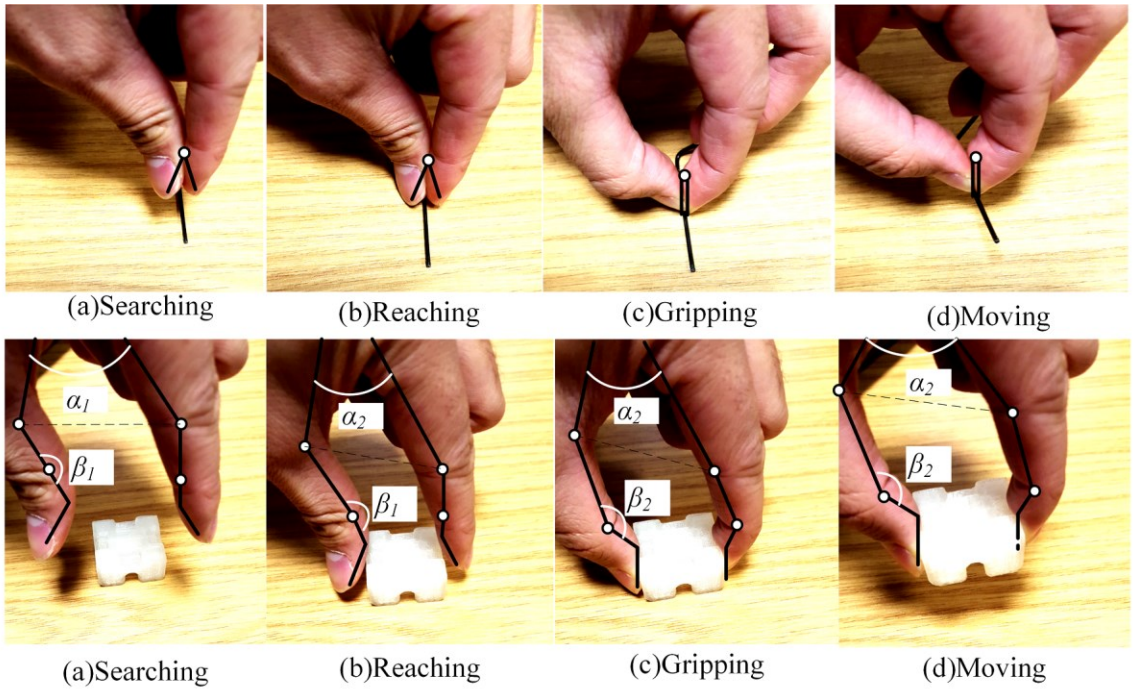
(a)Searching
(b)Reaching
(c)Gripping
(d)Moving
α_1
β_1
α_2
β_1
α_2
β_2
α_2
β_2
(a)Searching
(b)Reaching
(c)Gripping
(d)Moving

Fig.4

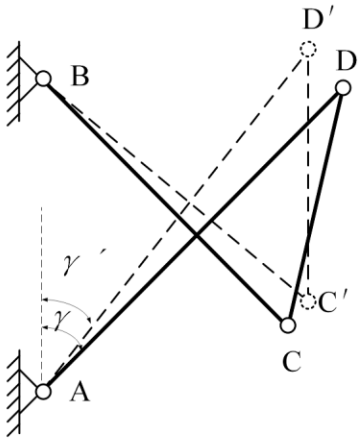

(a) CFB mechanism

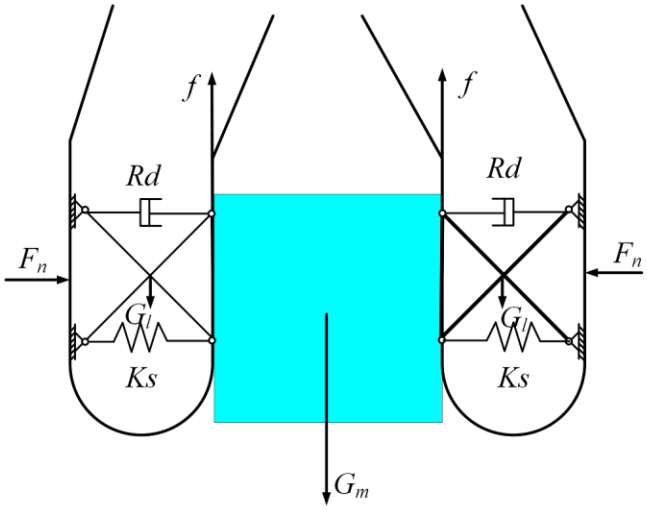

(b) CFB-damper-spring components

Fig. 5

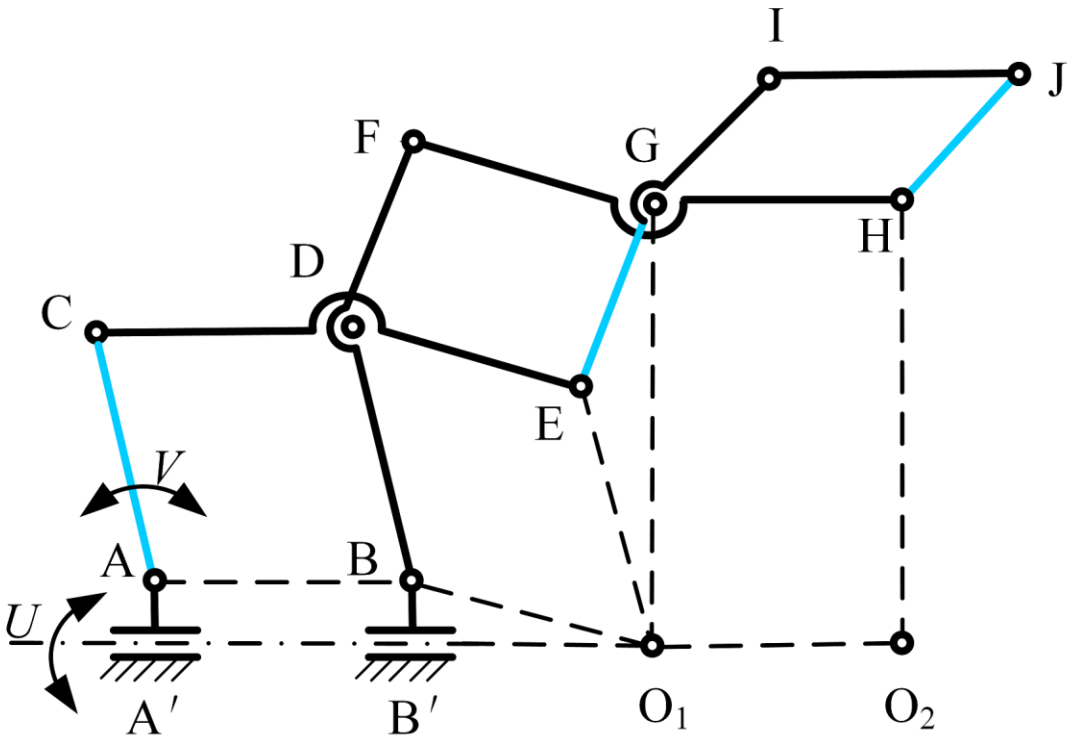

Fig. 6

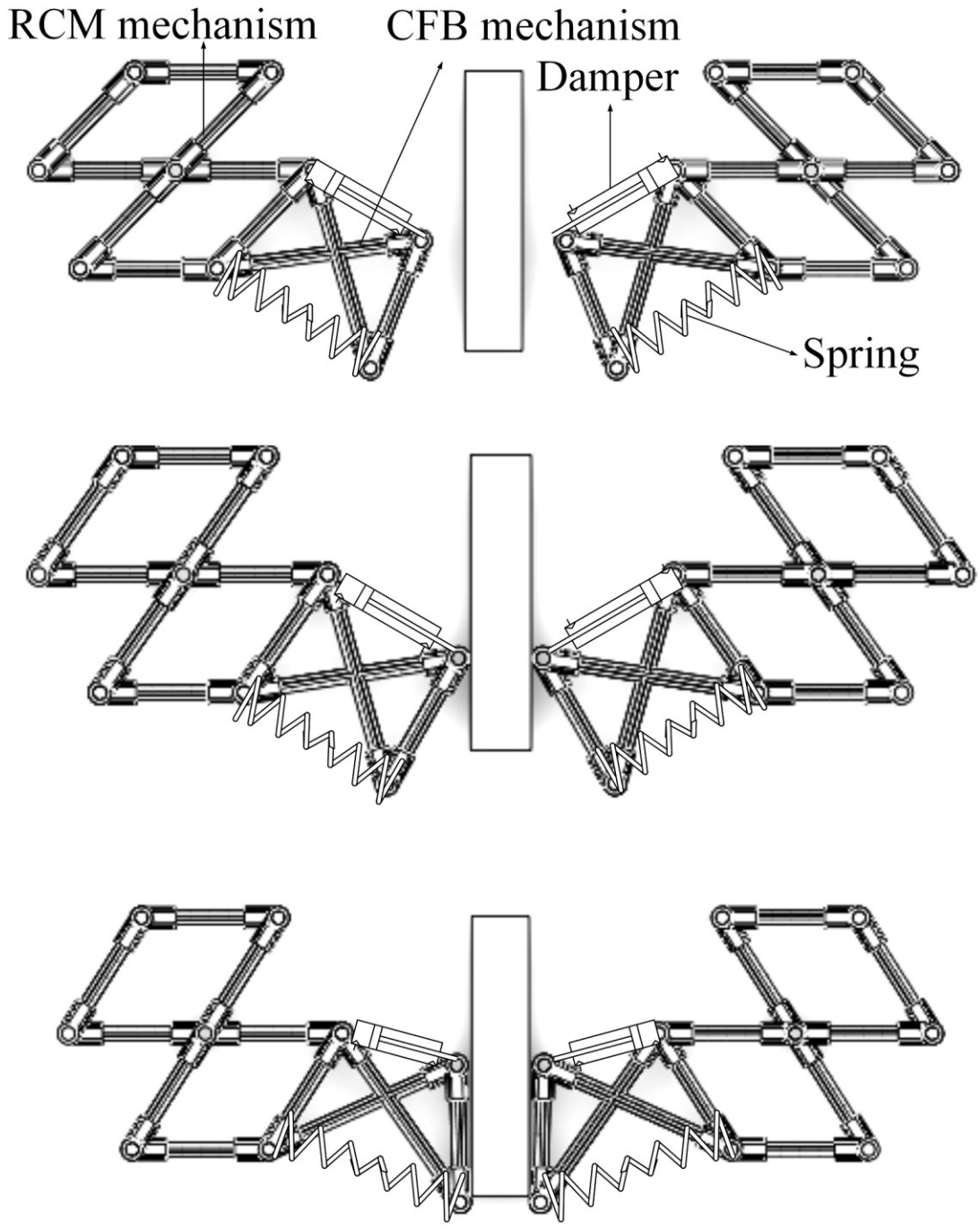

Fig. 7

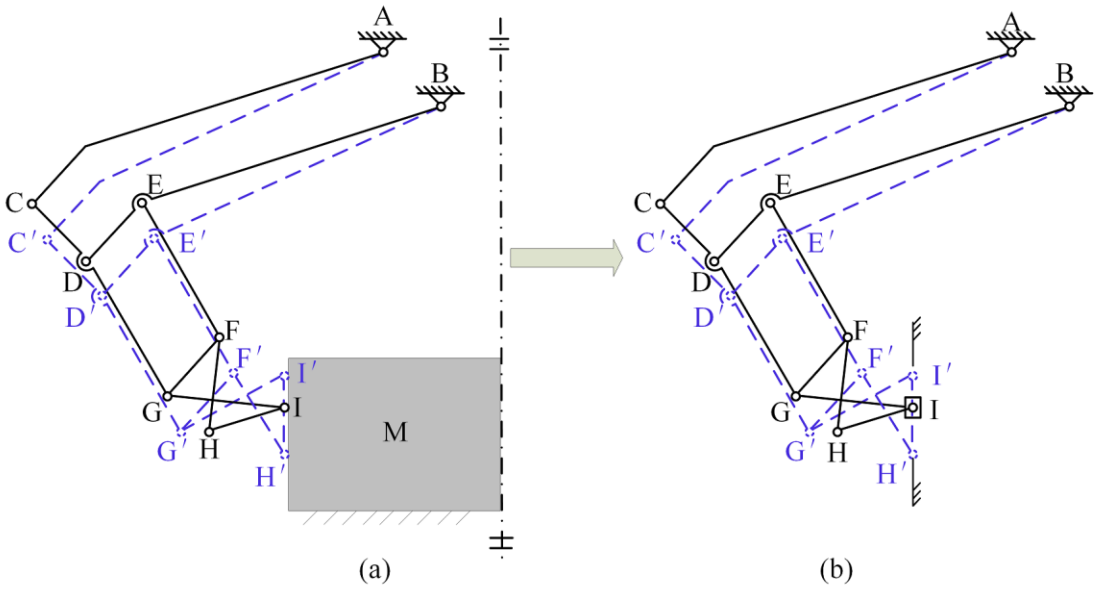

Fig. 8

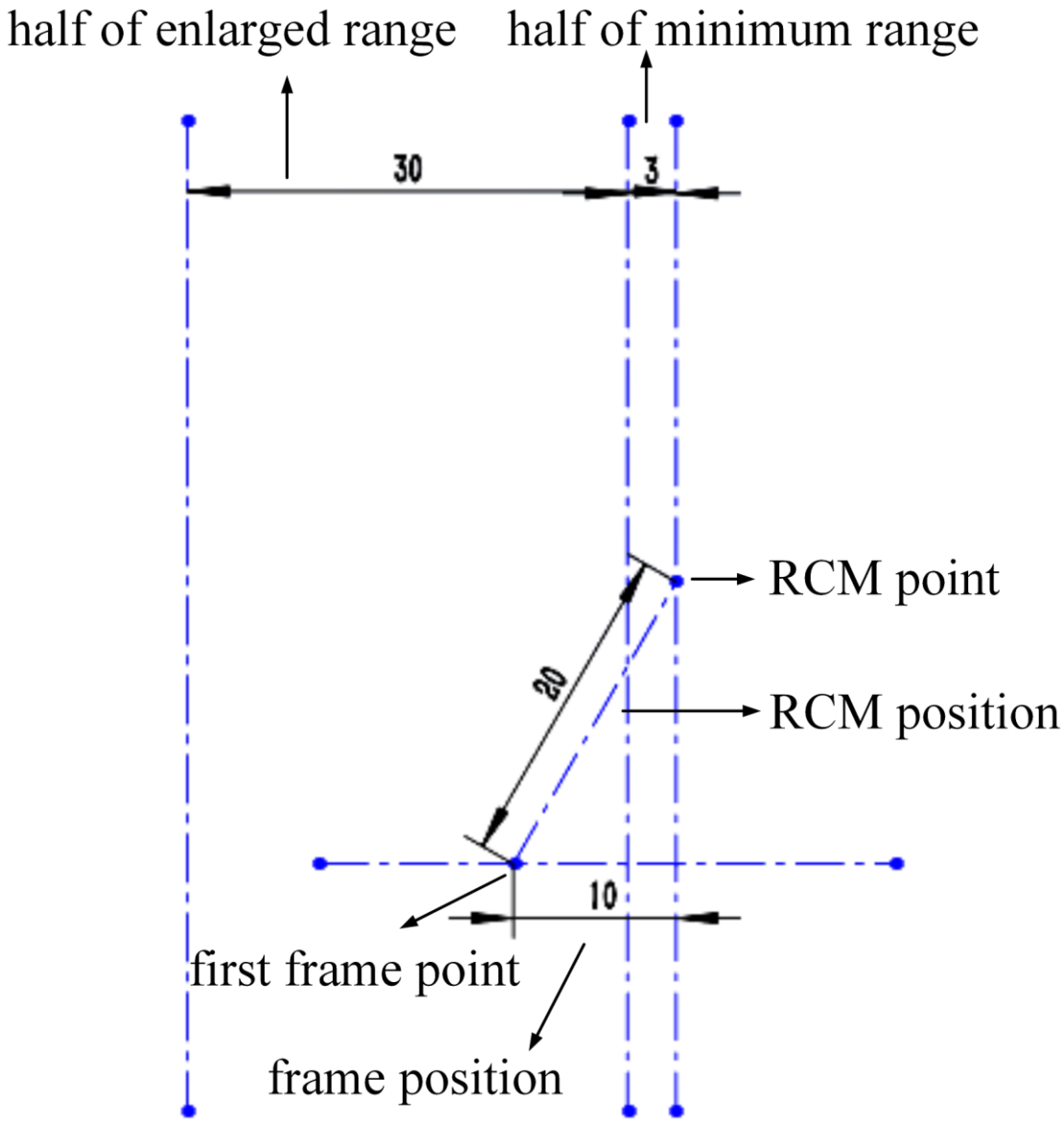
half of enlarged range
half of minimum range
30
3
RCM point
20
RCM position
10
first frame point
frame position

Fig. 9

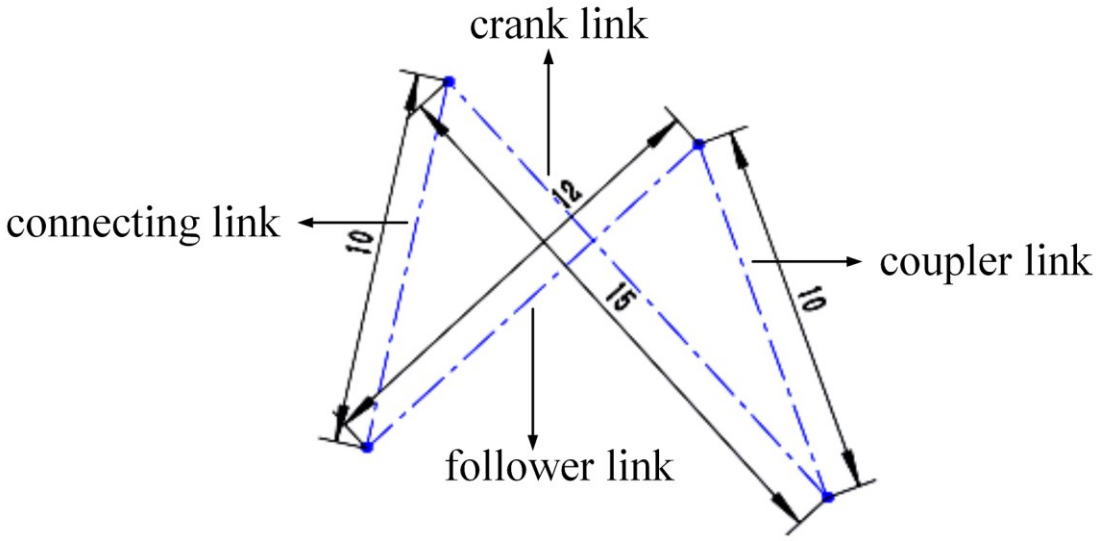
crank link
connecting link
coupler link
follower link
12
10
15
10

Fig. 10

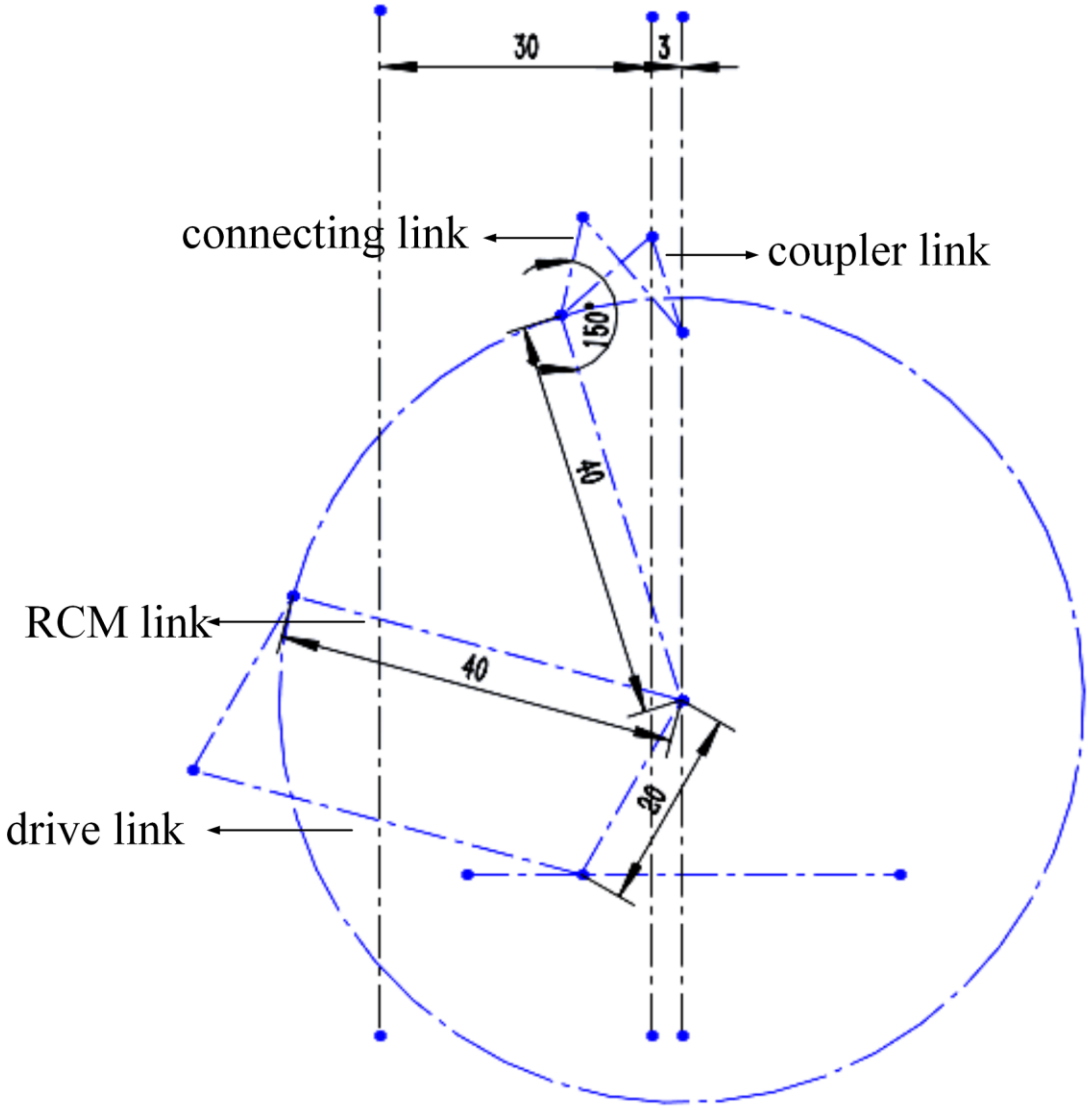
30
3
connecting link
coupler link
150°
40
RCM link
40
drive link
20

Fig. 11

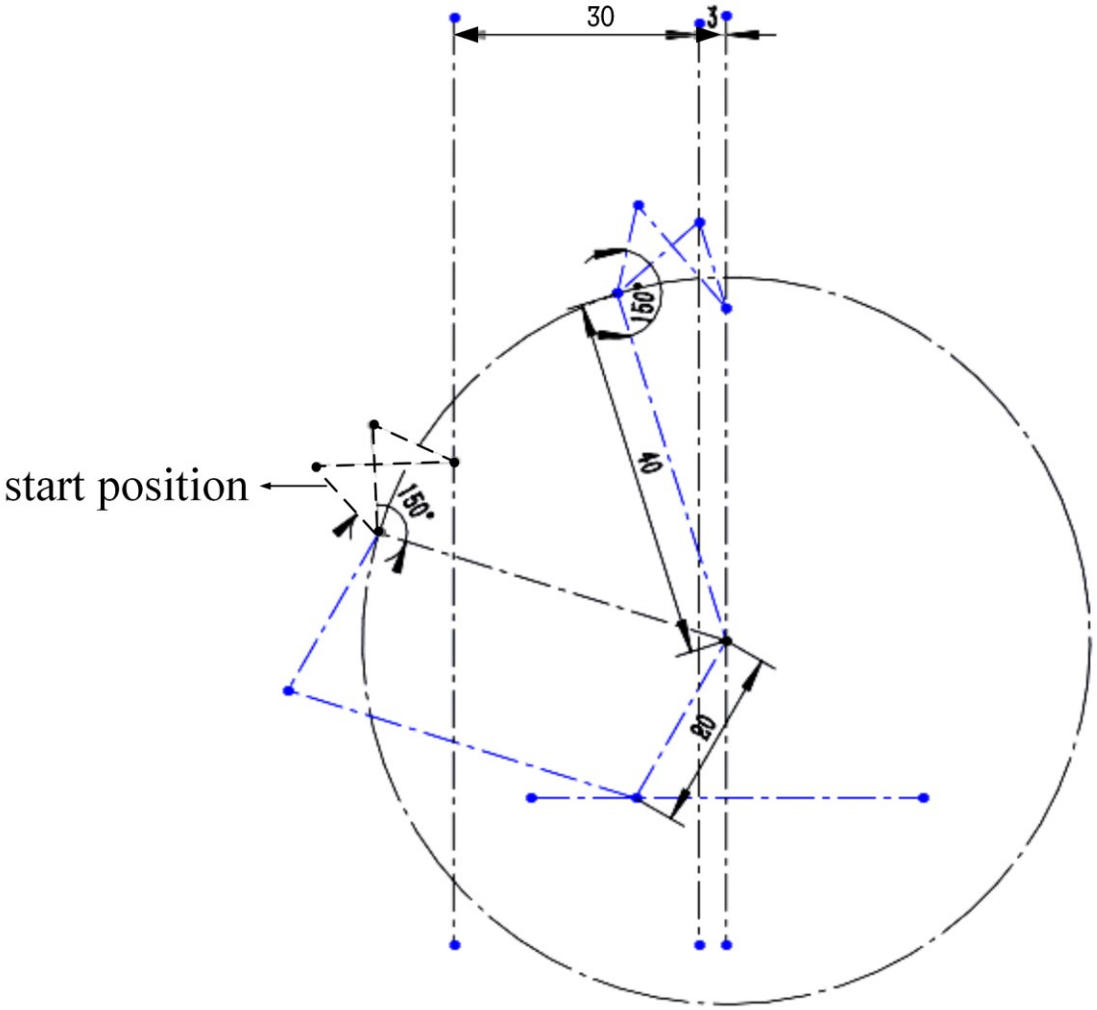

Fig. 12

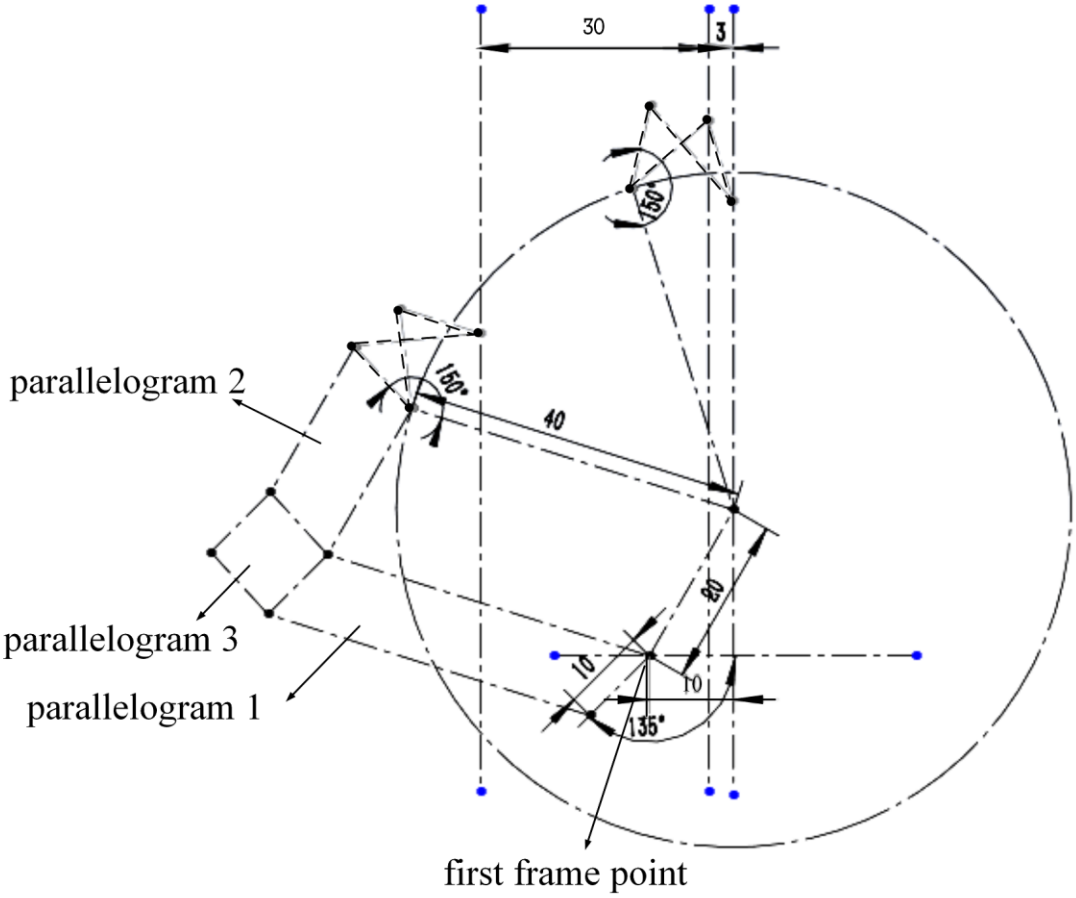
30
3
150
150°
40
parallelogram 2
20
parallelogram 3
10
10
parallelogram 1
135°
first frame point

Fig. 13

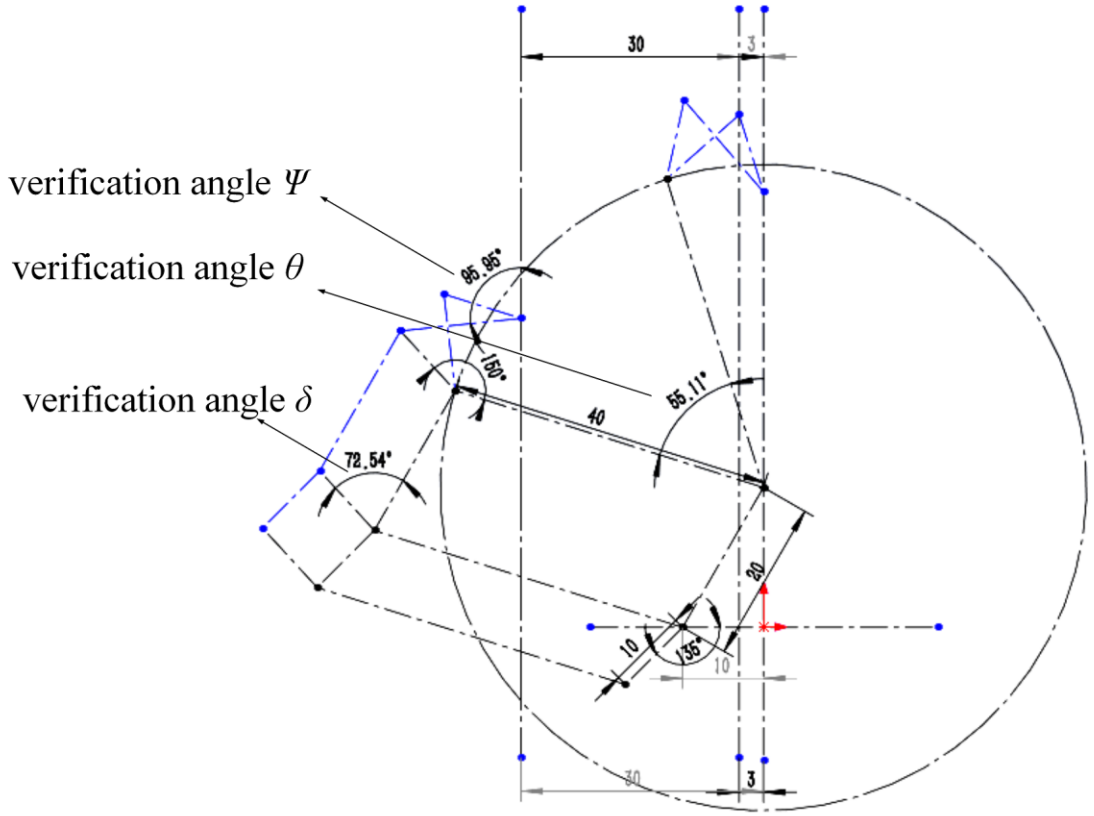
verification angle Ψ
verification angle θ
verification angle δ
30
3
95.95°
150°
55.11°
40
72.54°
20
10
135°
10
30
3

Fig. 14

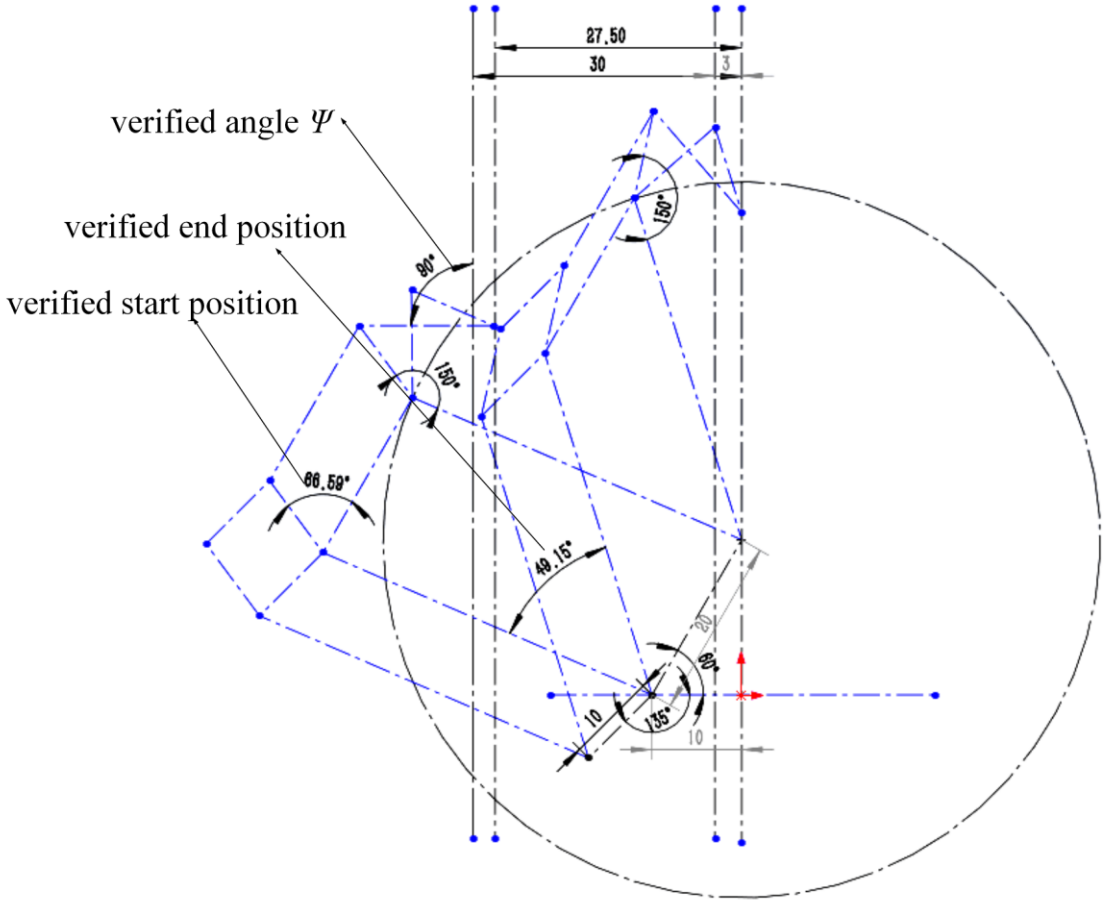
27.50
30
3
verified angle Ψ
verified end position
verified start position
90°
150°
150°
66.59°
49.15°
20
60°
10
135°
10

Fig. 15

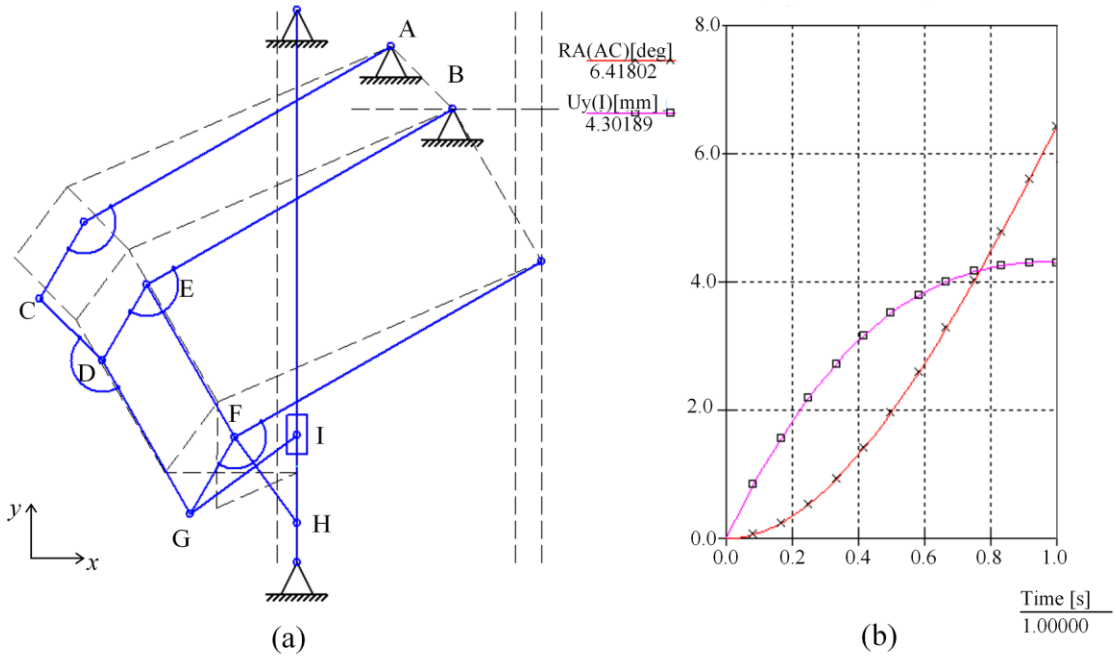
A
B
C
D
E
F
G
H
I
y
x
RA(AC)[deg]
6.41802
Uy(I)[mm]
4.30189
8.0
6.0
4.0
2.0
0.0
0.0
0.2
0.4
0.6
0.8
1.0
Time [s]
1.00000

(a) (b)

Fig. 16

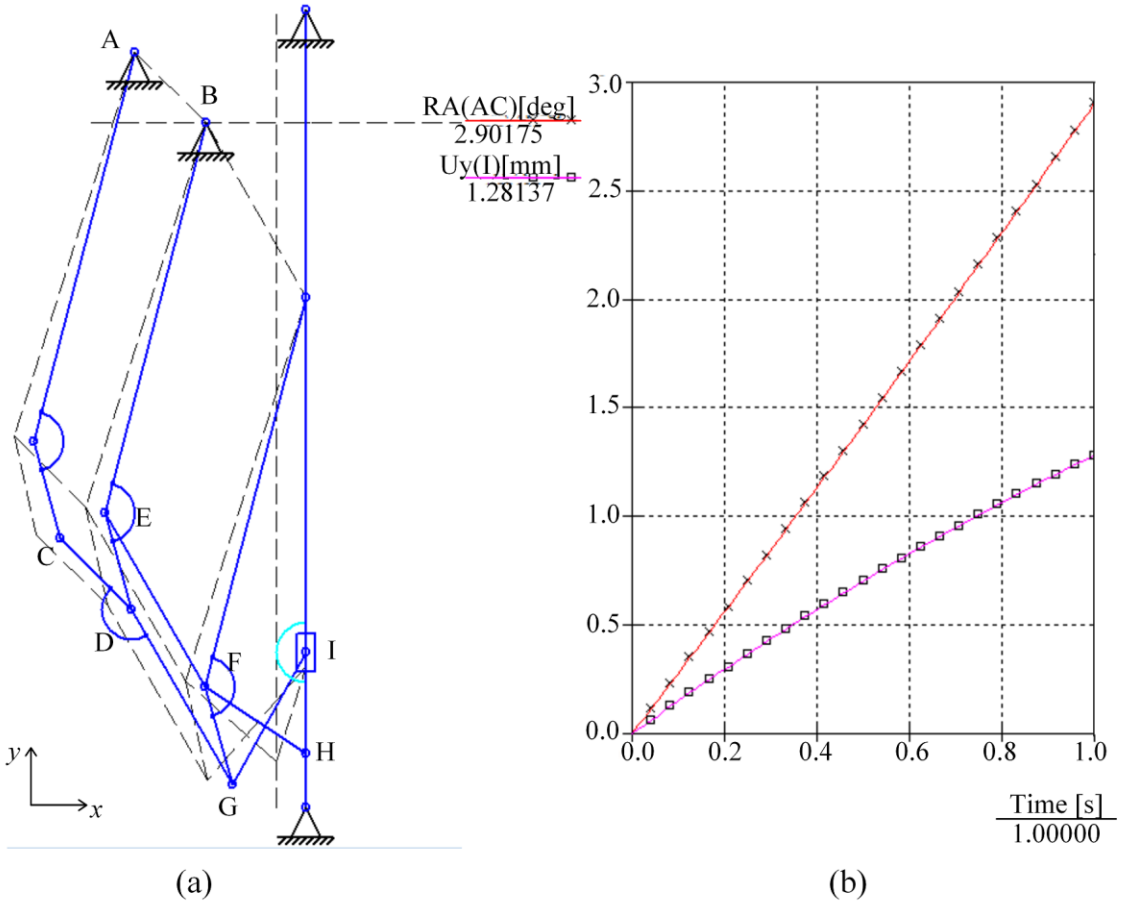
A
B
C
D
E
F
G
H
I
y
x
RA(AC)[deg]
2.90175
Uy(I)[mm]
1.28137
3.0
2.5
2.0
1.5
1.0
0.5
0.0
0.0
0.2
0.4
0.6
0.8
1.0
Time [s]
1.00000

(a) (b)

Fig. 17

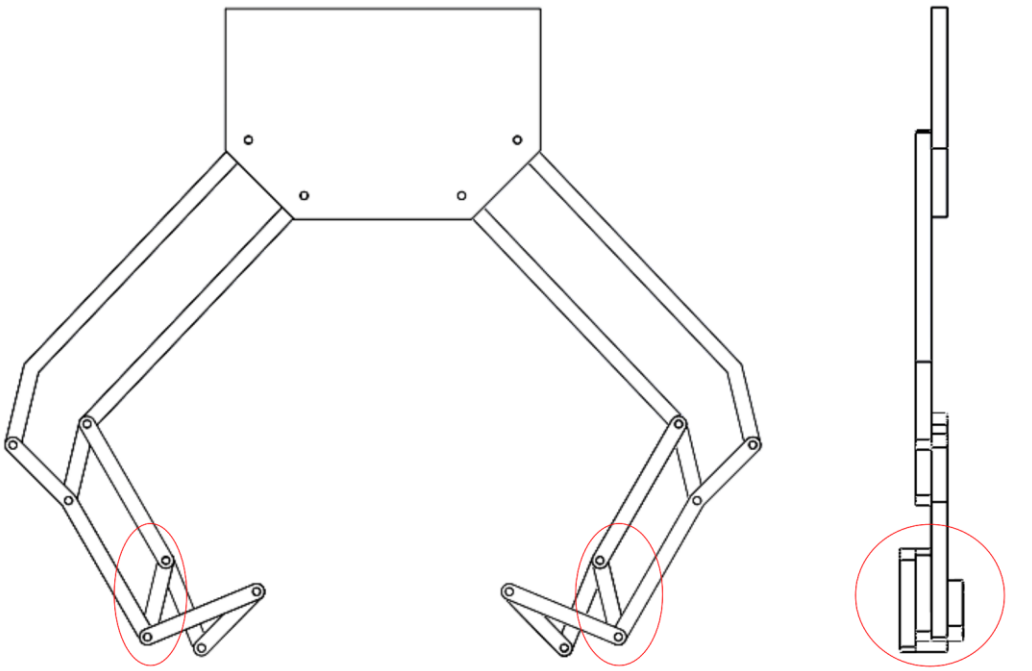

(a) front view (b) side view

Fig. 18

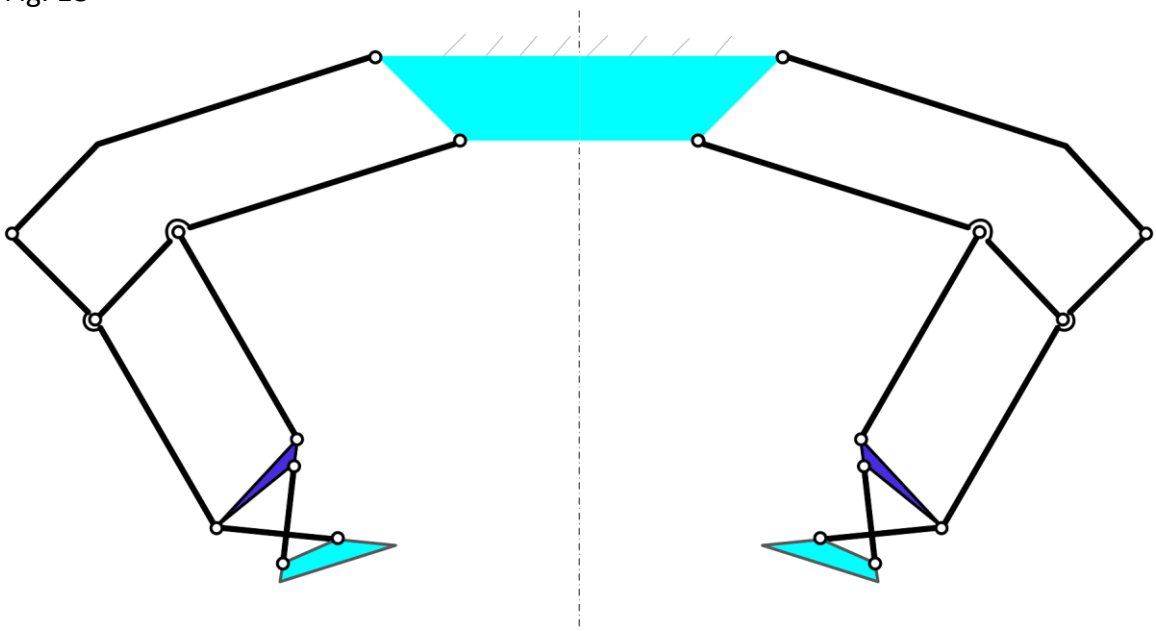

Fig. 19

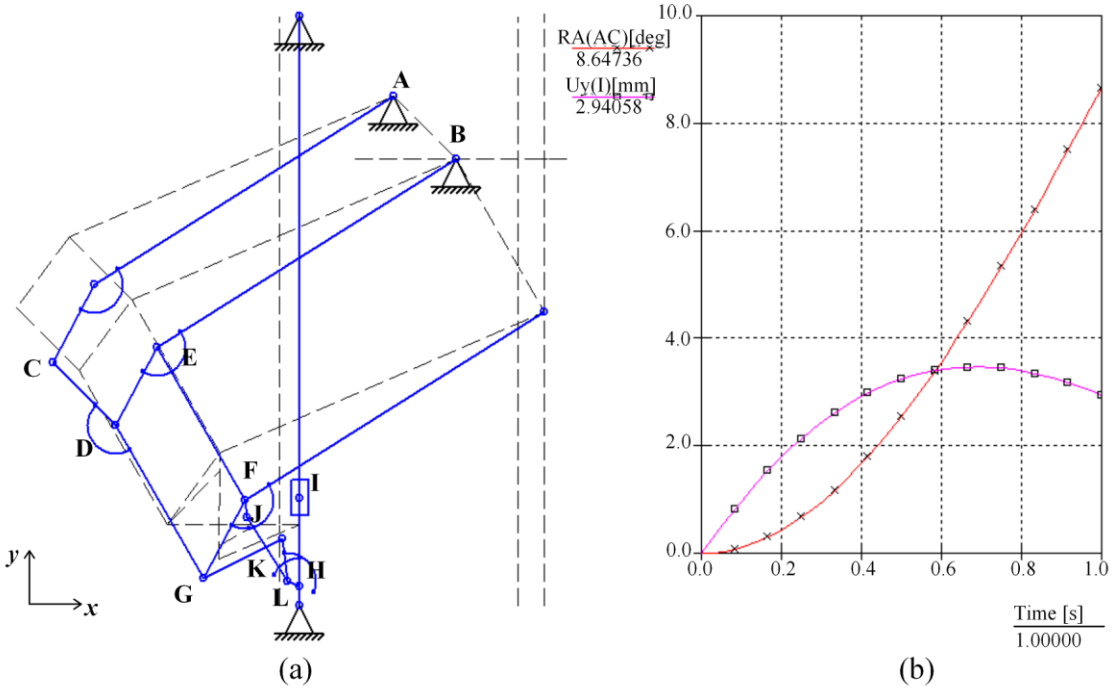
A
B
C
D
E
F
G
H
I
J
K
L
y
x
RA(AC)[deg]
8.64736
Uy(I)[mm]
2.94058
10.0
8.0
6.0
4.0
2.0
0.0
0.0
0.2
0.4
0.6
0.8
1.0
Time [s]
1.00000

(a) (b)

Fig. 20

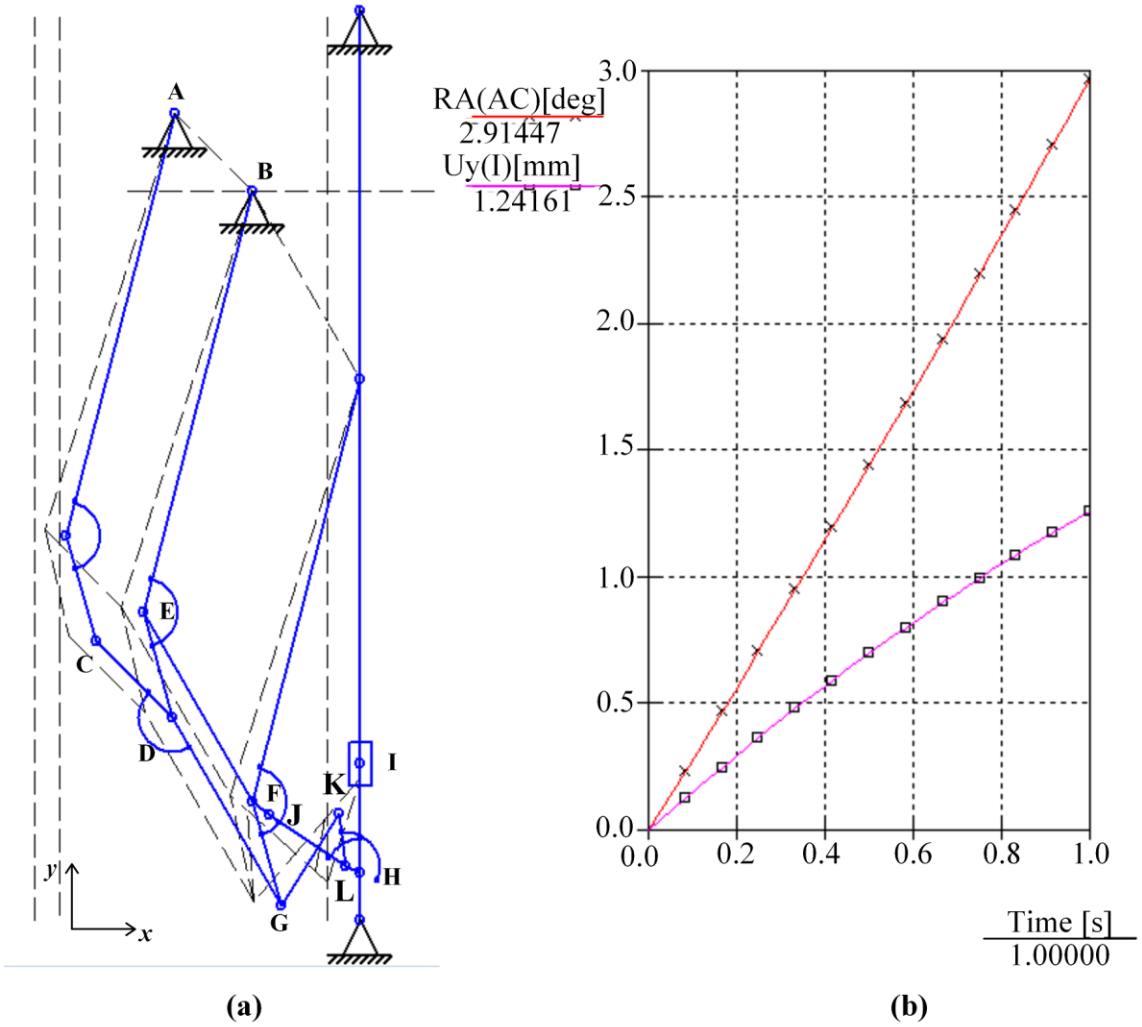
A
B
C
D
E
F
G
H
I
J
K
L
y
x
RA(AC)[deg]
2.91447
Uy(I)[mm]
1.24161
3.0
2.5
2.0
1.5
1.0
0.5
0.0
0.0
0.2
0.4
0.6
0.8
1.0
Time [s]
1.00000
(a)
(b)

Fig. 21

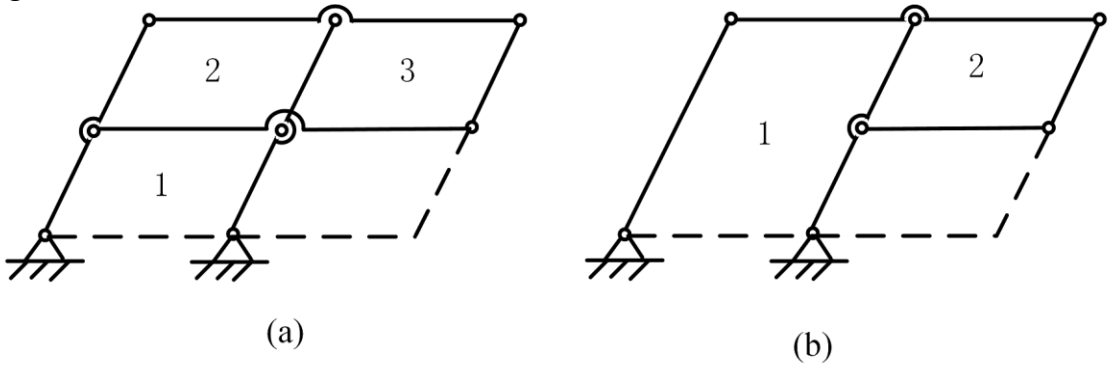

Fig. 22

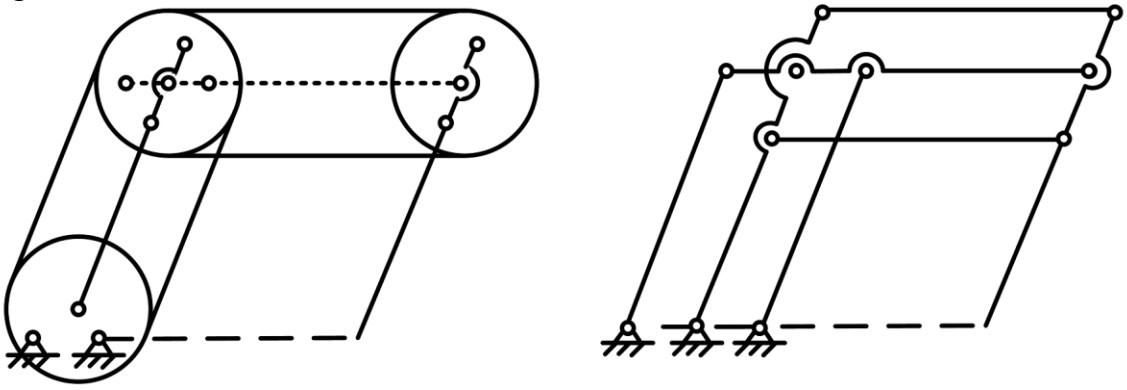

(a) (b)

Fig. 23

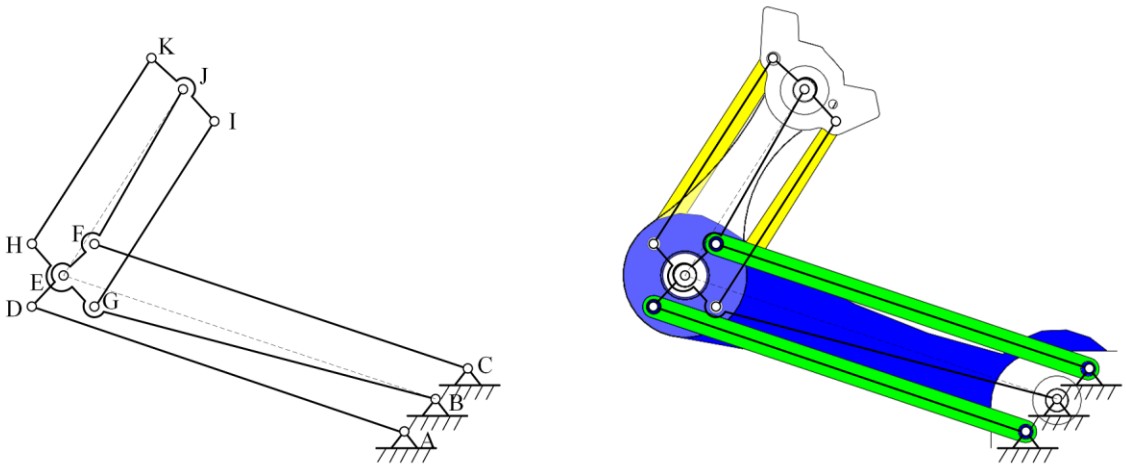

(a) (b)

Fig. 24

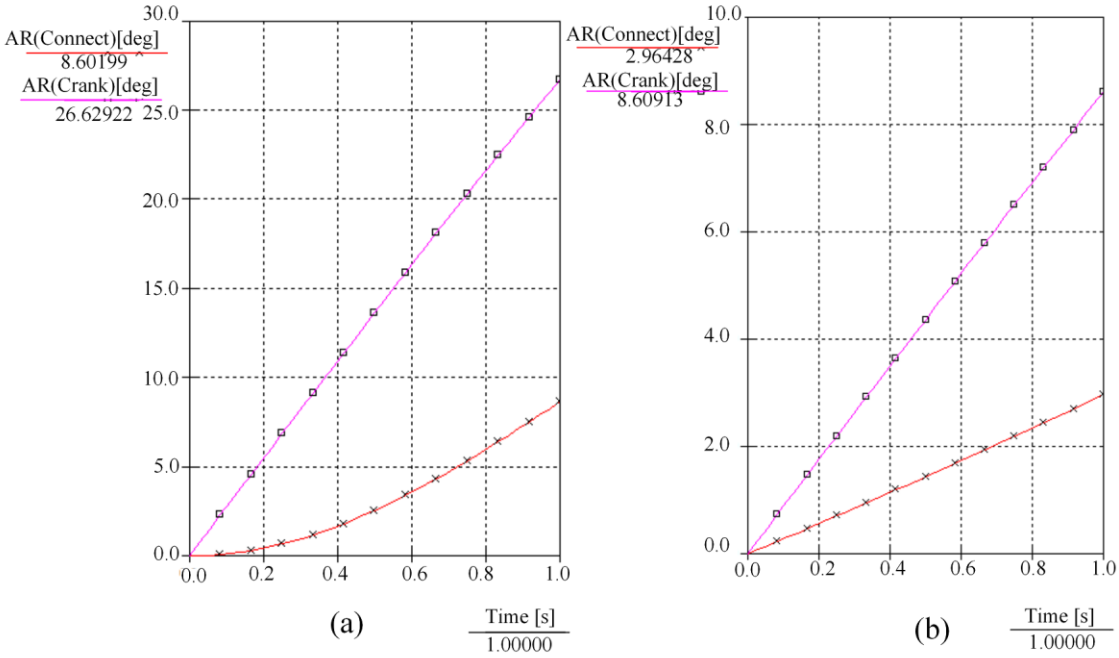
AR(Connect)[deg]
8.60199
AR(Crank)[deg]
26.62922
30.0
25.0
20.0
15.0
10.0
5.0
0.0
0.0
0.2
0.4
0.6
0.8
1.0
(a)
Time [s]
1.00000
AR(Connect)[deg]
2.96428
AR(Crank)[deg]
8.60913
10.0
8.0
6.0
4.0
2.0
0.0
0.0
0.2
0.4
0.6
0.8
1.0
(b)
Time [s]
1.00000

Fig. 25

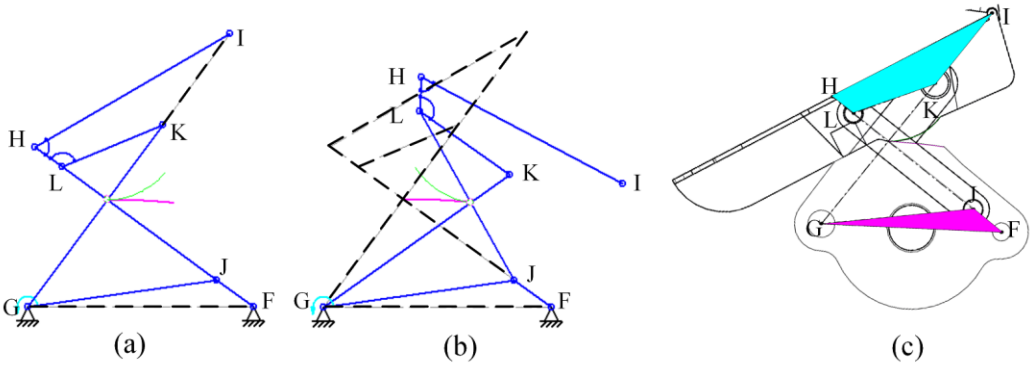

Fig.26

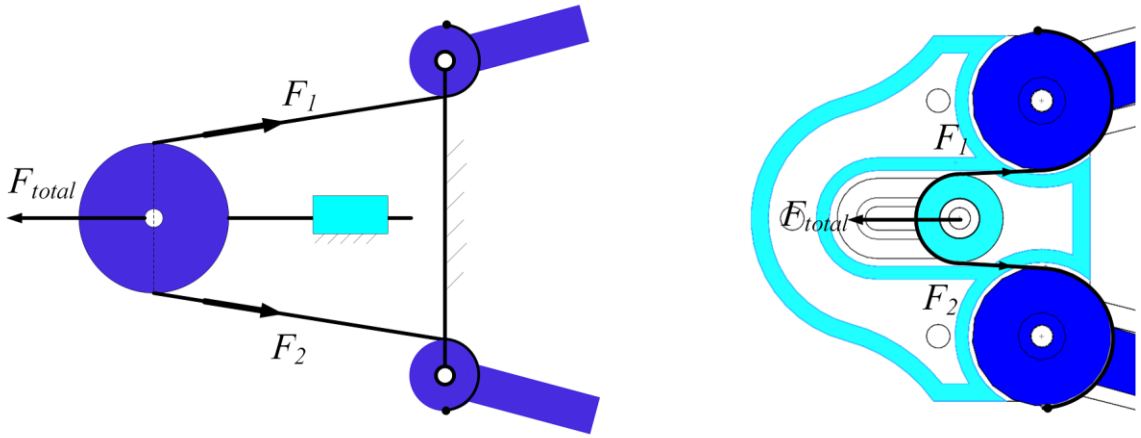

Fig. 27

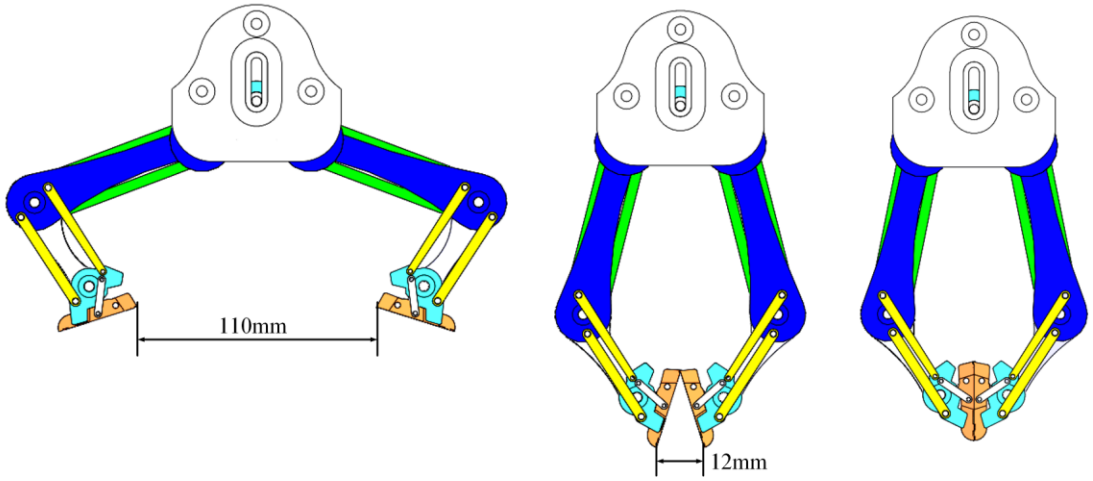

Fig. 28a

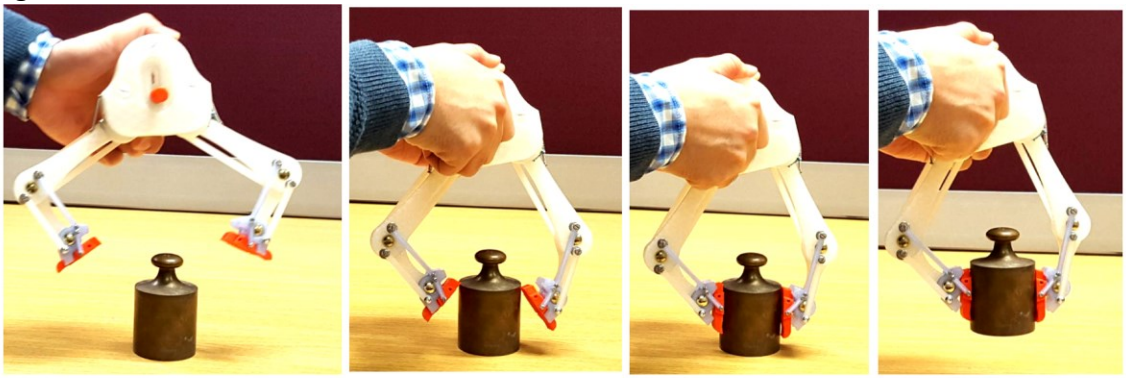

(a) Weight, 1Kg, dimensions: Φ50mm*55mm

Fig.28b

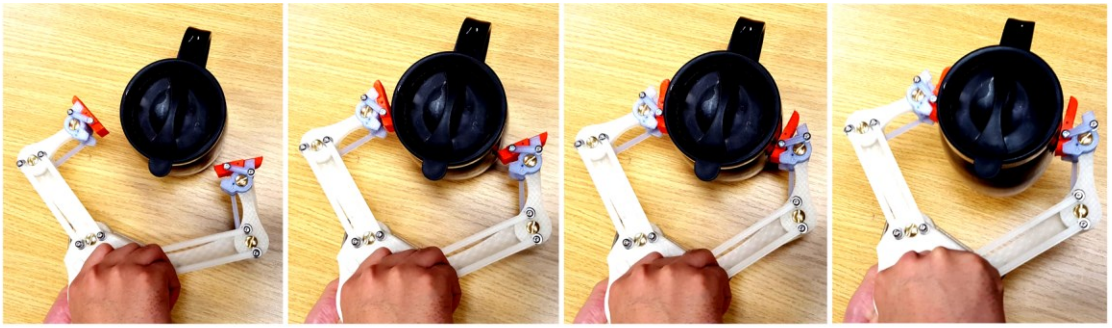

(b) Café cup, 450g, dimensions: Φ105mm*120mm

Fig.28c

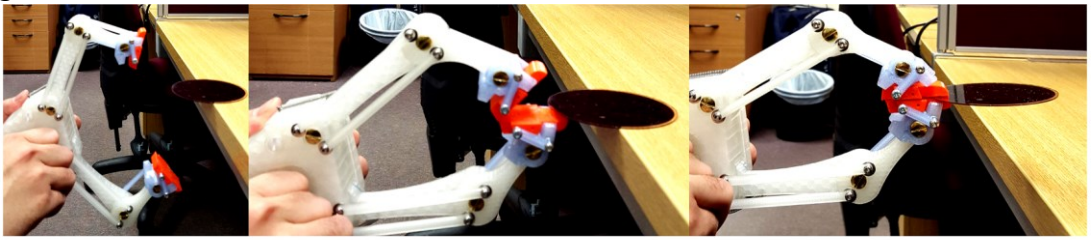

(c) Wafer, 9.5g, dimensions: Φ76mm*0.8mm

Fig.28d

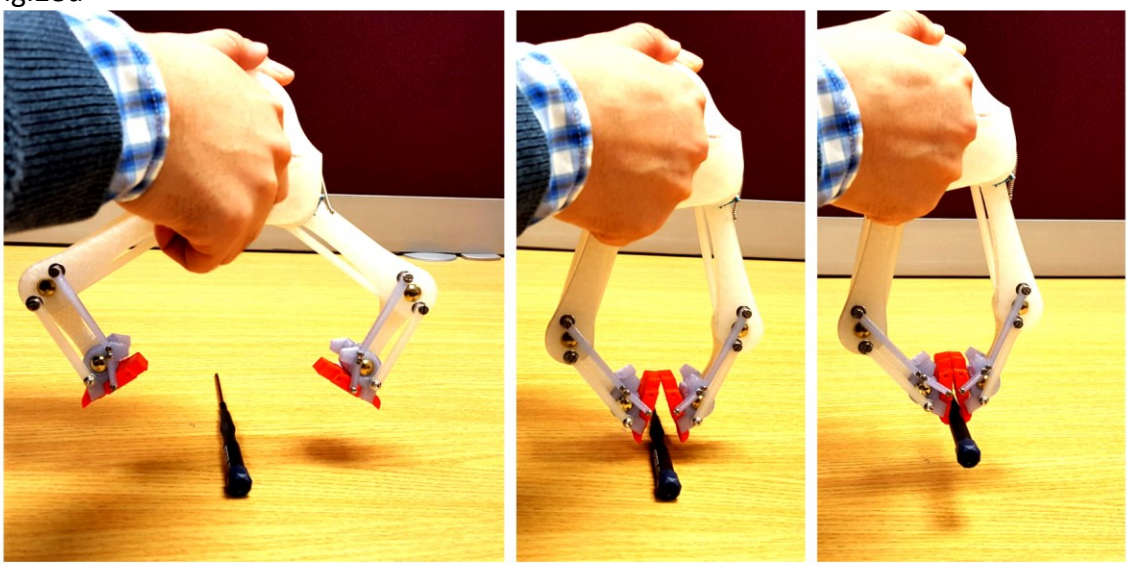

(d) Screw driver, 12g, dimensions: Φ7mm-Φ10mm

Fig.28e

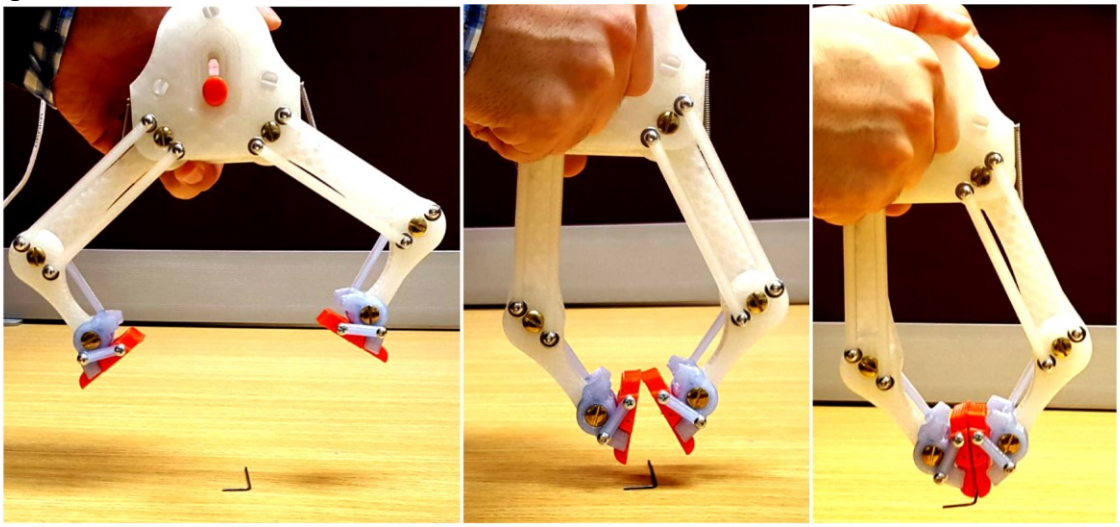

(e) Hex wrench, 0.5g, dimension: Φ1.5mm

Fig.28f

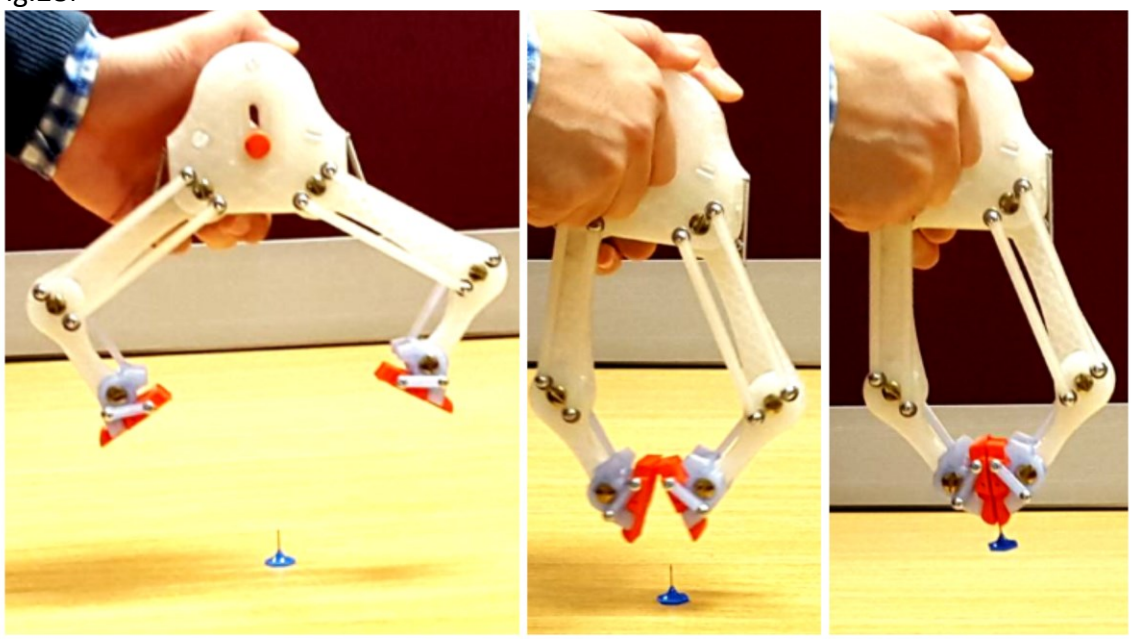

(f) Stick pin, 0.5g, dimensions: Φ0.5mm-Φ1mm

Fig.28g

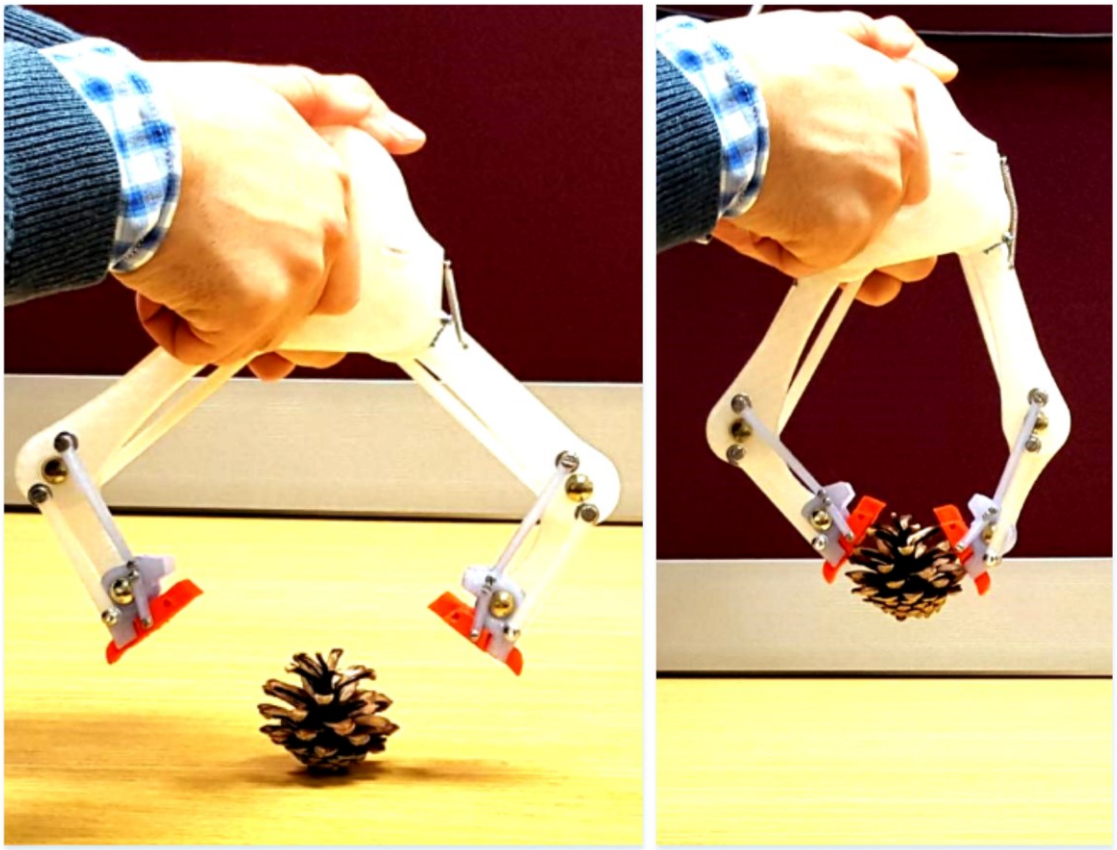

(g) Pinecone, 10g, irregular shape